

Separation of CO₂/CH₄ using Mixed Matrix Membranes



By

Taha Abbas Bin Rashid

School of Chemicals & Materials Engineering (SCME)

National University of Sciences & Technology (NUST)

2017

Separation of CO₂/CH₄ using Mixed Matrix Membranes



Name: Taha Abbas Bin Rashid

Reg. No: 00000118741

**This work is submitted as a MS thesis in partial fulfillment of
the requirement for the degree of**

(MS in Chemical Engineering)

Supervisor Name: Dr. Arshad Hussain

School of Chemicals & Materials Engineering (SCME)

National University of Sciences & Technology (NUST)

September, 2017

Certificate

This is to certify that work in this thesis has been carried out by Mr. **Taha Abbas Bin Rashid** and completed under my supervision in Memar laboratory, School of Chemical and Materials Engineering, National University of Sciences and Technology, H-12, Islamabad, Pakistan.

Supervisor: _____

Prof. Dr. Arshad Hussain

Chemical Engineering Department

National University of Sciences and

Technology, Islamabad

Submitted through

Principal/Dean,

Chemical Engineering Department

National University of Sciences and Technology, Islamabad

Dedication

To my father and mother

Acknowledgments

First of all, I would like to thank Almighty Allah for His blessings and helped me to complete this work. I would also like to express my sincere gratitude to my supervisor Prof. Dr. Arshad Hussain for his guidance, patience and motivation throughout this research work.

I would like to thank my guidance and examination committee (GEC) members Dr. Sarah Farrukh and Dr. Bilal Khan Niazi for their valuable guidance.

Also, my appreciation goes to my family and friends for their encouragement, love and support throughout my life.

Abstract

Polyamide 6 is a very tough polymer having high tensile strength. It is also highly resistant to chemicals which makes it very good candidate for gas separation. In this research CO₂/CH₄ gas permeation behavior was observed for flat sheet polymeric membrane. The membranes were formed by solution casting method. Multi walled Carbon nanotubes were subsequently added to observe the permeability of CO₂ relative to CH₄. The morphology of Mixed Matrix membranes (MMM) were observed through Scanning Electron Microscope (SEM). However, MMM were further characterized by Thermo Gravimetric Analysis (TGA), X-ray Diffraction (XRD) and Universal Tensile Testing machine (UTM). Carbon nanotubes were homogeneously dispersed in Nylon 6 polymer. The permeation experiments were performed to find the permeation behavior of both gases in pure polymeric membrane and MMM membrane. Experiments demonstrated very high permeability and at low pressure for polymeric membranes. The membranes however showed insignificant selectivity.

Keywords: cellulose acetate, multi walled CNT, carbon dioxide, methane

Table of Contents

Chapter – 1 Introduction	1
Background	1
Basic theory of membrane	1
Modes of membrane processes	3
1.1.1. In-line filtration.....	3
1.1.2. Cross-flow filtration	4
Types of membrane processes	4
1.4.1. Classification by nature	4
1.4.2. Classification by morphology.....	5
Application of membrane processes	8
1.5.1. Microfiltration (MF).....	8
1.5.2. Ultrafiltration (UF)	9
1.5.3. Reverse Osmosis (Hyperfiltration).....	9
1.5.4. Nanofiltration.....	9
1.5.5. Gas Separation.....	10
Chapter – 2 Literature Review	11
2.1. Membrane Technology for gas separation.....	11
2.2. Selection of Polymer and Membrane Preparation	12
2.3. Facilitated Transport Membranes	14
2.4. Fixed Site Carrier Membranes.....	14
2.5. Mixed Matrix Membranes (MMM).....	15
2.6. Objective	16
Chapter – 3 Experimental Methods	17
3.1. Materials	17

3.2.	Solution Preparation.....	17
3.3.	Membrane Casting.....	18
3.4.	Permeation Testing Apparatus.....	18
3.4.1.	Equipment Description.....	18
3.4.2.	Instrumentation.....	18
3.4.3.	Working of Gas Permeability Test system.....	19
Chapter – 4 Resources and Approaches.....		20
4.1.	Characterization Techniques.....	20
4.1.1.	Scanning Electron Microscopy (SEM):.....	20
4.1.1.1.	Components of SEM.....	20
4.1.1.2.	Working principle.....	21
4.1.1.3.	Magnification in SEM:.....	21
4.1.1.4.	Quality of the Image.....	22
4.1.1.5.	Image formation.....	22
4.1.2.	Thermal Gravimetric Analysis (TGA).....	22
4.1.2.1.	Instrumentation.....	22
4.1.2.2.	Working principle.....	24
4.1.2.3.	Types of thermogravimetry.....	24
4.1.2.4.	Factors affecting TGA curve.....	24
4.1.2.5.	Information obtained from TGA.....	24
4.1.3.	Mechanical Testing.....	24
4.1.3.1.	Universal Testing Machine (UTM).....	25
4.1.3.2.	Working principle.....	25
4.1.4.	X-ray Diffraction (XRD).....	26
4.1.4.1.	Instrumentation.....	26

4.1.4.2.	Working principle	27
4.1.4.3.	Applications	27
Chapter – 5	Results and Discussions	28
5.1.	Scanning Electron Microscopy (SEM)	28
5.2.	Gas Permeation Study	30
5.2.1.	Thickness Adjustment of membranes.....	30
5.2.2.	Addition of MWCNTs in PA6 Membrane in Formic Acid.....	31
5.2.2.1.	Results	32
5.2.3.	Addition of MWCNTs in PA6 Membrane in Phenol	40
5.2.3.1.	Results	41
5.2.4.	Effect of pressure difference on gas permeability	49
5.2.5.	Effect of temperature on gas permeability and selectivity	52
5.2.6.	Effect of filler loading on gas permeability and selectivity.....	53
5.3.	X-Ray Diffraction (XRD)	54
5.4.	Thermogravimetric Analysis	56
5.5.	Tensile Testing.....	58
5.6.	Conclusion	61
5.7.	Future Recommendations	62
Appendix – A	63
References	64

List of Figures

Figure 1: Membrane Schematics	3
Figure 2: In-line filtration	3
Figure 3: Cross-flow filtration	4
Figure 4: Classification of Synthetic membranes	5
Figure 5: Microporous membrane	6
Figure 6: Dense membrane	6
Figure 7: Electrically charged membrane	7
Figure 8: Loeb-Sourirajan membranes (left) and thin film composite membranes (right). 7	
Figure 9: Liquid membranes	8
Figure 10: Robeson upper bound curve	12
Figure 11: Gas Permeability Test System.....	18
Figure 12: Schematics of scanning electron Microscope	21
Figure 13: Schematics of Thermal Gravimetric Analysis.....	23
Figure 14: Universal Testing Machine (UTM).....	26
Figure 15: X-Ray Diffractometer Schematics	26
Figure 16: Surface Morphology and Cross section a pure membrane, c 10wt% CNTs under 30 μm , e 10wt% CNTs above 50 μm (Surface Morphology) b pure membrane, d 10wt% CNTs under 30 μm , f 10wt% CNTs above 50 μm (Cross Section)	29
Figure 17: Permeabilities of CO_2 and CH_4 at different Temperatures.....	32
Figure 18: Permeabilities of MWCNTs/PA6 membranes in Formic Acid.....	34
Figure 19: Selectivities of MWCNTs/PA6 membranes in Formic Acid	36
Figure 20: Permeabilities of MWCNTs/PA6 membranes in Formic Acid.....	37
Figure 21: Selectivities of MWCNTs/PA6 membranes in Formic Acid	39
Figure 22: Permeabilities of MWCNTs/PA6 membranes in Phenol	42
Figure 23: Selectivities of MWCNTs/PA6 membranes in Phenol	44
Figure 24: Permeabilities of MWCNTs/PA6 membranes in Phenol	46
Figure 25: Selectivities of MWCNTs/PA6 membranes in Phenol	48
Figure 26: Effect of pressure difference on permeability ($T = 65\text{ }^\circ\text{C}$)	49
Figure 27: Effect of pressure difference on permeability ($T = 70\text{ }^\circ\text{C}$)	50
Figure 28: Effect of pressure difference on permeability ($T = 75\text{ }^\circ\text{C}$)	51

Figure 29: Effect of pressure difference on permeability (T = 80 °C)	51
Figure 30: Effect of Temperature on permeability	53
Figure 31: X-Ray Diffraction of pure PA6 membrane at T = 65 C.....	54
Figure 32: X-Ray Diffraction of pure PA6 membrane at T = 70 C.....	55
Figure 33: X-Ray Diffraction of pure PA6 membrane at T = 80 C.....	55
Figure 34: TGA Analysis of pure PA6 membrane synthesized at 70 °C	57
Figure 35: TGA Analysis of pure PA6 membrane synthesized at 75 °C	57
Figure 36: TGA Analysis of pure PA6 membrane synthesized at 80 °C	58
Figure 37: Stress vs Strain relationship of 10 wt% MWCNTs in phenol, Pure PA6 membrane, 10 wt% MWCNTs in Formic Acid.....	59
Figure 38: Tensile Strength of different membrane materials	59
Figure 39: % Elongation of different membrane materials	60

List of Tables

Table 1: Comparison of different membrane processes	10
Table 2: Pure PA 6 membranes of different thickness	30
Table 3: MWCNTs in PA6 with different wt % of PA6 in Formic Acid	31
Table 4: Permeabilities of CO ₂ and CH ₄ at different Temperatures	32
Table 5: Permeabilities of MWCNTs/PA6 membranes in Formic Acid	33
Table 6: Selectivities of MWCNTs/PA6 membranes in Formic Acid.....	35
Table 7: Permeabilities of MWCNTs/PA6 membranes in Formic Acid	37
Table 8: Selectivities of MWCNTs/PA6 membranes in Formic Acid	38
Table 9: MWCNTs in PA6 with different wt % of PA6 in Phenol	40
Table 10: Permeabilities of MWCNTs/PA6 membranes in Phenol	41
Table 11: Selectivities of MWCNTs/PA6 membranes in Phenol.....	43
Table 12:Permeabilities of MWCNTs/PA6 membranes in Phenol	45
Table 13: Selectivities of MWCNTs/PA6 membranes in Phenol.....	47
Table 14: Effect of Temperature on Permeability and Selectivity	52
Table 15: Mechanical Properties of different Membrane Materials.....	61

Abbreviations

Polyamide 6 (PA6)

Multi-walled Carbon Nano Tubes (MWCNTs)

Formic Acid (FA)

Cellulose Acetate (CA)

Poly Ethylene Glycol (PEG)

Mixed Matrix Membrane (MMM)

Scanning Electron Microscopy (SEM)

Universal Tensile Machine (UTM)

XRay Diffraction (XRD)

Thermogravimetric Analysis (TGA)

Micro Filtration (MF)

Ultra Filtration (UF)

Reverse Osmosis (RO)

Nano Filtration (NF)

Gas Separation (GS)

Polyethylene Oxide (PEO)

Facilitated Transport Membrane (FTM)

Fixed Site Carrier Membranes (FSC)

Metal Organic Frameworks (MOF)

Sulfonated poly (ether ether ketone) (S-PEEK)

Chapter – 1

Introduction

Background

Monsanto manufactured the first successful industrial gas separation membrane in 1979-1980. Hydrogen was separated from a mixture of argon, nitrogen and methane. The separation was an easy one and economical one. This encouraged Monsanto to install several dozen systems worldwide.

Since the 1980s gas separation membranes have been utilized for variety of separation processes like carbon dioxide separation from methane and separation of hydrogen from refinery streams. Air separation into its component gases is also very demanding process for offshore installations. On a smaller scale, membranes are also used for many other applications like in Dialysis

The search for better membrane materials is going on for many decades but results have been disappointing most of the time. Despite synthesis of thousands of new materials, more than 90% of commercial membranes are being manufactured from fewer than 10 membrane materials.

Commercially all membrane materials are polymeric and separate gas mixtures by solution diffusion mechanism. Membrane technology is already in use in large parts of world for desalinating seawater. Carbon capture and storage is being increasingly in use in many industries to mitigate climate change. Membrane technology is one of the possible contender for capturing CO₂. The development of inorganic and polymeric membrane having high selectivity and permeability is needed [1].

Basic theory of membrane

Membrane separation is a technique based on the separation of component gases by controlling their permeabilities. There are two underlying models used to describe permeation mechanism:

1. Pore flow model
2. Solution diffusion model

In pore flow model, permeation is done by driving force of pressure difference. Here flow is convective flow. Separation is achieved because one of the component specie is filtered out through pores while the other one cannot.

The second model is solution-diffusion model. This model shows that first permeant adsorbs on membrane surface and then diffuses through the membrane material due to concentration difference. The separation of components is due to difference of their solubilities in membranes and differences in their diffusivities through membrane material. These two models were proposed in nineteenth century but pore flow model became popular in 1940s because of its close resemblance to physical phenomena. After mid 1940s solution diffusion model was being used to explain gas transport through polymeric materials. There was no controversy regarding solution diffusion model but mechanism of transport in reverse osmosis was debated largely throughout 1960s. After 1980s solution diffusion became the dominant model for the explanation of reverse osmosis in scientific community and very few scientists use pore flow model to explain reverse osmosis.

Diffusion is a process in which permeants are transported from one side of a membrane to other side by concentration difference. Individual molecules of permeant specie are in completely random motion in a membrane material and they have no specific preference for any direction. Although average displacement of molecule can be calculated after specified period of time nothing can be said about the direction in which it will move. However, if concentration gradient is established across membrane surface then it will move from region of high concentration to low concentration.

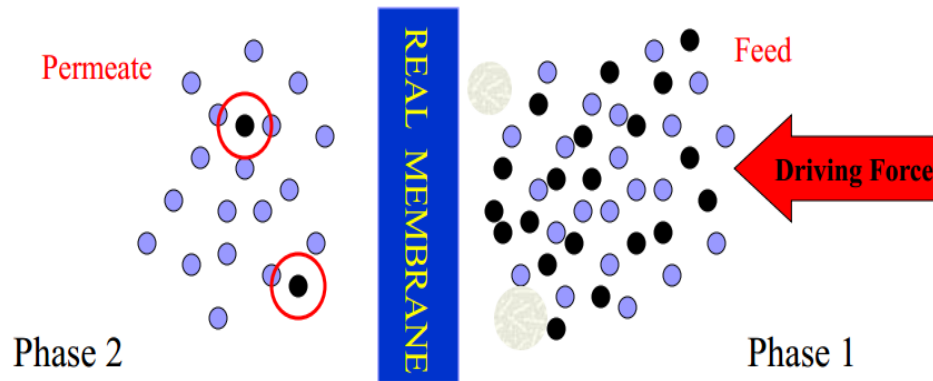


Figure 1: Membrane Schematics

Modes of membrane processes

There are two modes of operation in membrane technology. It depends on the direction of flow relative to membrane surface.

1.1.1. In-line filtration

In-line filtration also known as dead-end filtration is flow in which entire volume of fluid is forced to pass through membrane under the influence of pressure. As the accumulation of particle increases on the membrane surface, the pressure which is required to maintain flow also increases. After some point, membrane will be clog and must be replaced.

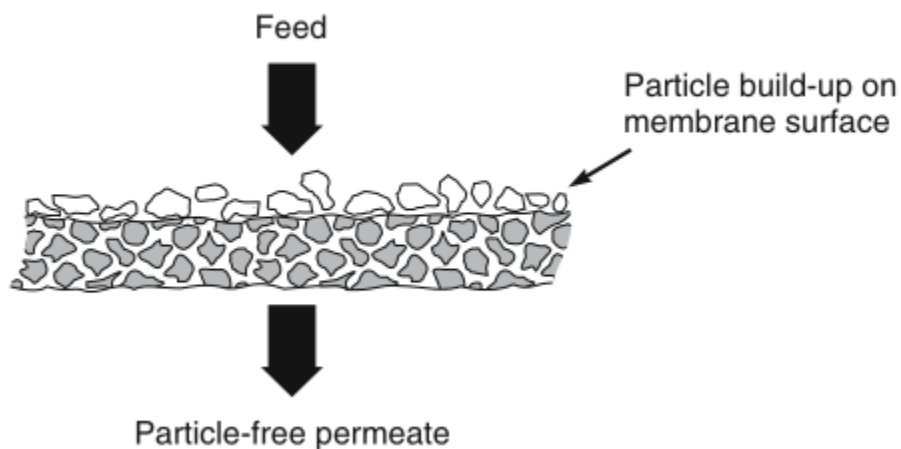


Figure 2: In-line filtration

1.1.2. Cross-flow filtration

In cross-flow mode of transport, feed solution circulates at the top of membrane surface resulting in two output streams. One is impurity free permeate stream, the other one is concentrate which contains excess of impurities. The cross-flow filtration is achieved through much complex equipment compared to in-line flow but life time of equipment is more than that of in-line flow. Flow stream having concentration of solid particles less than 0.1% is always treated in in-line membranes whereas streams having solid concentration greater than 0.5% is always treated in cross flow membranes. Between these two concentration any membrane can be used depending on the nature of solid material and its application [3].

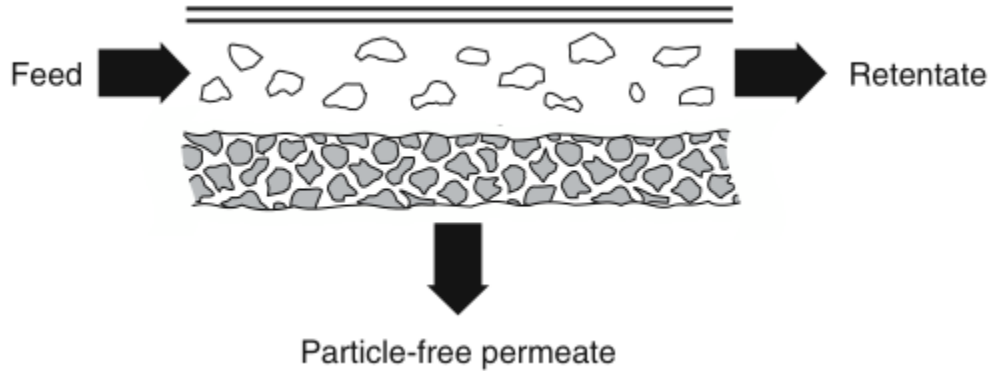


Figure 3: Cross-flow filtration

Types of membrane processes

Classification of membranes is based on

- I. Nature of membrane
- II. Morphology of membrane

1.4.1. Classification by nature

- I. Biological membranes: (living and non-living)
- II. Synthetic (organic and inorganic)

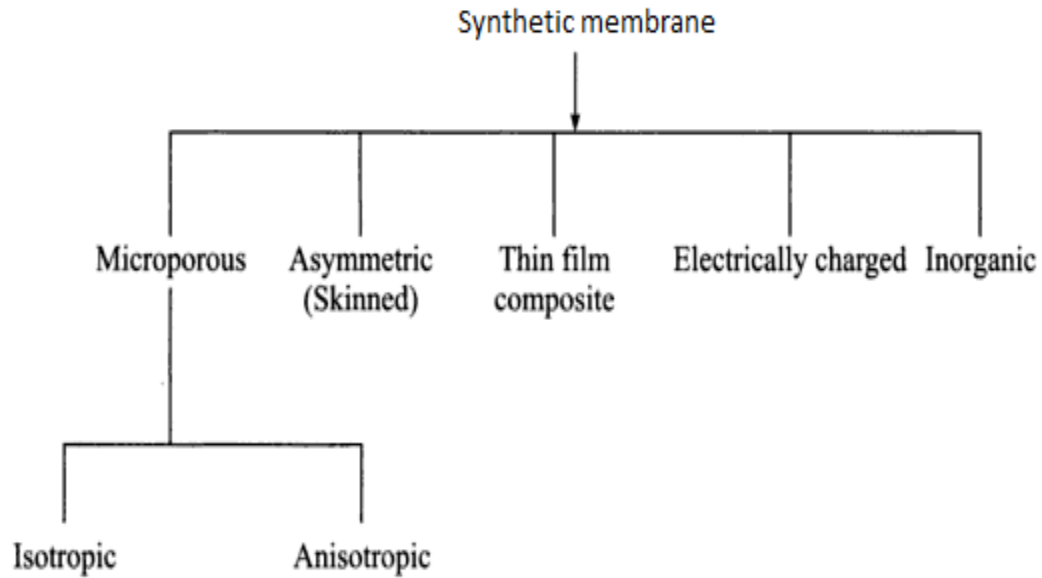


Figure 4: Classification of Synthetic membranes

1.4.2. Classification by morphology

Membranes are further classified by morphology into

- I. Isotropic membranes
- II. Anisotropic membranes

1.1.2.1. Isotropic membranes

Isotropic membranes also have following types:

- I. Microporous membranes
- II. Nonporous, Dense membranes

1.1.2.1.1. Microporous membranes

Microporous membranes are similar to conventional filter. It has very high number of voids. However, the size of pores varies compared to conventional filter. They are in the range of 0.01 – 10 μm in diameter. Particles smaller than larger pores but larger than smaller pores are rejected partially according to pore size distribution. Therefore, the separation of solute from microporous membrane depends upon size of molecule and pore size distribution.

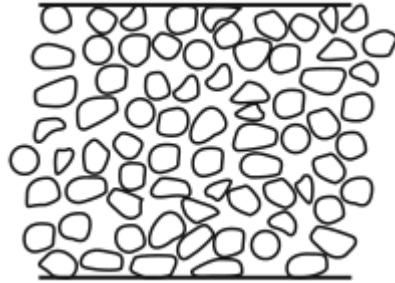


Figure 5: Microporous membrane

1.1.2.1.2. Non-porous, Dense membranes

Dense membranes consist of a film where pore size is less than 1nm. In these membrane solutes pass under the influence of driving force. Driving force is different in different scenarios. Driving force can be pressure difference, concentration difference, and electrical potential gradient. Separation of various components is based on their relative transport rate through membrane. Relative rate depends on two factors: Diffusivity and Solubility.



Figure 6: Dense membrane

1.1.2.1.3. Electrically charged membranes

These membranes can be microporous or dense but mostly they are microporous with their walls containing positive or negative charges. Membrane with fixed positive charges is categorized as anion exchange membrane while the one with fixed negative charges is categorized as cation exchange membrane. Anion exchange membrane will attract negative charges while cation exchange membrane will attract positive charges. Separation is dependent on two factors: Ion concentration in solution and charge of ion. Therefore,

monovalent ions are less likely to be separated than divalent ions. These membranes are used in electro dialysis.

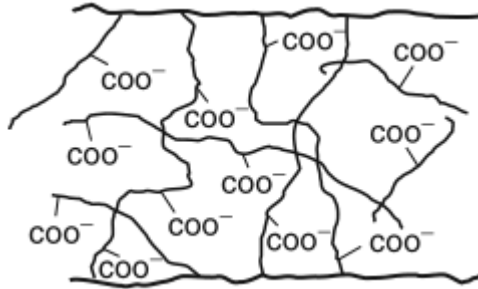


Figure 7: Electrically charged membrane

1.1.2.2. Anisotropic membranes

In membranes, rate of transport of a component specie depends on membrane thickness. Highly thick membrane will have low transport rate whereas thin membrane will have high transfer rate. Conventionally to produce defect free and mechanically strong membrane, film thickness is limited to 20 μm . Anisotropic membranes have a characteristic of having very thin dense layer on top of thick porous membrane. Porous membrane provides support while dense layer provides separation. Thus, porous membrane increases permeability while dense layer increases selectivity. Therefore, flus is so great that it is used in almost every commercial membrane [4].

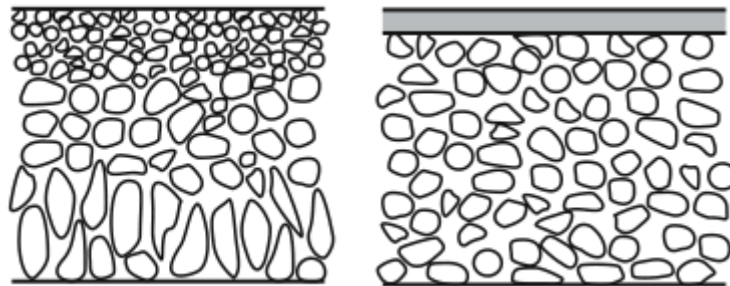


Figure 8: Loeb-Sourirajan membranes (left) and thin film composite membranes (right)

1.1.2.3. Metal, Ceramic and liquid membranes

Mostly membranes used so far are polymeric membranes but now interest in membrane materials is increasing. Ceramic membranes are microporous membranes being increasingly used in ultrafiltration. Ceramics offer high thermal stability and resistance to corrosive solvents. Dense metal membranes are used in various separation processes. For instance, hydrogen is being separated from gaseous mixtures with palladium membranes. Liquid membranes are another category of membranes. They are mostly used for carrier facilitated transport processes.

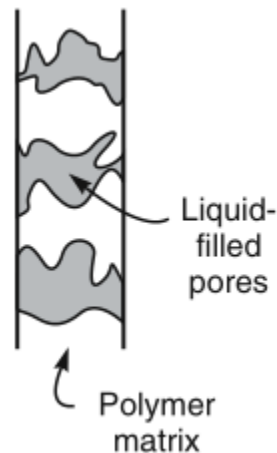


Figure 9: Liquid membranes

Application of membrane processes

1.5.1. Microfiltration (MF)

Microfiltration is a process to remove suspended and colloidal particles having size larger than $0.08 - 2 \mu\text{m}$. It operates within pressure range of $0.05 - 0.1 \text{ MPa}$. It is similar in to coarse filtration used to remove suspended solids. Pore size is in the range of $0.1 - 10$ microns. Materials used for the formation of microfiltration membranes are Cellulose acetate, polyethersulfone (PES), polysulfone (PS), zirconia, alumina etc. Microfiltration membranes can have the following industrial applications

- I. Waste water treatment
- II. Fruit juice clarification
- III. Metal recovery
- IV. Separation of oil/water emulsions.

1.5.2. Ultrafiltration (UF)

This process lies between nanofiltration and microfiltration. Pore size varies from 0.05 μm to 1 μm . It is usually used for separation of large macromolecules from solution. Pressure varies from 0.07 MPa to 0.7 MPa. Applications of ultrafiltration includes:

- I. Carbohydrates and protein removal
- II. Recovery of oil, paint and surfactants from waste streams
- III. Fruit juices clarification

1.5.3. Reverse Osmosis (Hyperfiltration)

Reverse osmosis (RO) is most widely used membrane technology. Its main application is desalination of sea water. Regions of the world which have unusual period of drought utilize reverse osmosis to fulfill their potable water needs. Particle size should be larger than 0.001 μm . In reverse osmosis, driving force is pressure and it operates in the range of 2 – 10 MPa. Industrial applications include

- I. Desalination of sea water
- II. Production of ultra-pure water for utilization in semiconductor industry.

1.5.4. Nanofiltration

Nanofiltration membranes are sometimes used before RO membranes for treatment of sea water. They have low salt rejection but their biggest advantage comes in term of high permeability. They remove large contaminants whereas RO removes very fine contaminants mostly salts of sodium chloride. Therefore, they are also known as ‘loose Reverse Osmosis’ membranes. Usually divalent ions are rejected by nanofiltration whereas monovalent ions are removed by reverse osmosis. Common industrial applications include

- I. Removal of divalent ions from sea water.
- II. Pretreatment of sea water
- III. Removal of multivalent ions in dyes, herbicide and sugar industries
- IV. To produce ultra-pure water for semiconductor industry.

1.5.5. Gas Separation

In dense membranes, usually formed through solution casting technique, gas mixtures are made to pass through these membranes. Pressure difference works as a driving force.

Gas separation has application in many industries like:

- I. CO₂ separation and sequestration
- II. Enhanced oil recovery
- III. Air separation
- IV. Hydrogen separation
- V. Ammonia separation

Table 1: Comparison of different membrane processes

Sr. #	Membrane process	Membrane pore size (nm)	Driving force
1	Gas separation (GS)	< 1 nm	ΔP and ΔC
2	Reverse Osmosis (RO)	0.5 - 1	$\Delta P = 2 - 10$ MPa
3	Nanofiltration (NF)	In the range of nm	$\Delta P = 0.1 - 2$ MPa
4	Ultrafiltration (UF)	1 - 10	$\Delta P = 0.1 - 1$ MPa
5	Microfiltration (MF)	$10^2 - 10^4$	$\Delta P = 0.01 - 0.5$ MPa

Chapter – 2

Literature Review

2.1. Membrane Technology for gas separation

Gas separation is a very large industry. Particular application of membrane technology is gas sweetening. It is being done by many industries around the world for many years. Membrane process requires less energy, thereby less cost and has a feature of compactness. Due to compactness, it is mostly suitable for remote locations like offshore oil and gas rigs. It can be run on widely available source of energy which is electricity. Synthesis of energy efficient and cost efficient membranes is the key factor for their wide spread utilization. Two of the most important factors for gas separation membranes are their permeability and their selectivity. Various materials have been analyzed for the capture of carbon dioxide (CO₂). Ceramics plays a very important role in this but due to their high cost of synthesis they are mostly ruled out. For larger applications, polymeric materials are more suitable contender [5].

Polymeric materials are suitable because of their low-cost manufacturing and ease of synthesis. They can also be easily scaled up. Also, they require least amount of energy and maintenance. Membrane separation became economically competitive during 1970s and since then has always been more attractive for offshore applications. For on shore gas separation, investors tend to go for conventional technologies due to requirement of high cost energy (electricity) and also due to the fact that membrane module requires replacement every 2 – 4 years. CO₂/CH₄ has been at the forefront of gas separation technologies. Due to global awareness for protecting the environment, industries are under huge pressure from their respective governments for removal of greenhouse gases. CO₂ being one of the strong greenhouse gas is the largest contributor to global warming. Also, CO₂ natively present along with methane requires for its removal because it can cause huge loss in calorific value of methane, resulting in economic loss for industries and consumers alike. For this purpose, pure polymeric membranes or modified polymeric membranes are being investigated for CO₂ clean up.

In continental Europe, fossil fuel plants emitting CO₂ are major contributor for greenhouse effect. CO₂ is being emitted from exhaust gases into the atmosphere and their concentration is around 13%. Presence of other polluting gases along with CO₂ decreases the efficiency of membranes like SO_x and NO_x. CO₂ is of major concern for membranes because of its ability to cause plasticization thereby increasing permeability of every gas. This also results in decrease in selectivity.

2.2. Selection of Polymer and Membrane Preparation

The selection of polymeric materials for gas separation is based on various factors. Two of the factors are its permeability and selectivity. Other inherent polymer properties like toughness, elongation and abrasion resistance are also necessary. Wang et al. [6] obtained selectivity of CO₂ removal from methane of around 49 however it came at a cost of permeability which is very low of around 22.6 barrer. Jose et al. [7] obtained very high permeability of 3800 barrer but has very low selectivity of around 3.17. Usually a compromise has to be made between both as shown by Robeson [8]. Permeability and selectivity are inversely proportional to each other for polymeric membranes Fig. 10.

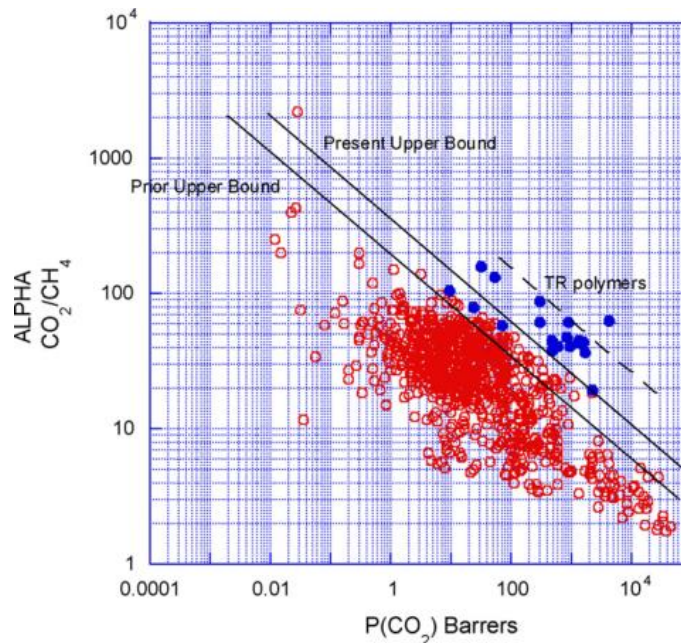


Figure 10: Robeson upper bound curve

Polyethylene oxide (PEO) is one contender for CO₂ capture due to oxygen presence which is polar in nature. Researchers have utilized different blends of PEO for CO₂ removal and

got very positive results. It is because of ethylene oxide linkage [10]. The major problem with these membranes is that they tend to crystallize after certain amount of time which reduces CO₂ permeability since crystal polymer has low permeability and high selectivity. This can be overcome by using branched chain PEO or low molecular weight of PEO. Nijmeijer et al. studied PEBAC 1074 for CO₂ separation has found better performance compared to other polymers. Polaris® is also one of the desirable polymers when it comes to CO₂ selectivity. Cellulose Acetate (CA) is an economical polymer having shown its performance repeatedly on an industrial scale. Research is ongoing for pure CA and its blends but pure CA is not suitable for CO₂ separation because of its low permeability and selectivity. Therefore, they also require modification in their structures or addition of binders and fillers for their efficient performance [9].

For membrane manufacturing many other techniques have been employed. Glassy polymers have been found to be better in terms of mechanical strength but have low % elongation, thus cannot be used where sudden pressure changes occur which can break membrane and will ultimately cause loss of product. Membrane thickness has an adverse effect on their permeability. Thick membranes have usually low permeability while thin membranes have high permeability. Thin membranes however require support material to sustain high pressure force. Loeb and Surirajan prepared asymmetrical membranes by combining high permeability of thin membranes with high mechanical strength of thick membranes. The thin selective layer has thickness of around 100 – 200 µm and is known as skin layer [10].

Membrane can differ in terms of their thickness from 0.1 – 0.5 µm prepared in laboratory to around 50 µm prepared by various companies for various industrial and commercial purposes. Robeson has done an extensive work in investigation of properties of different polymers regarding their selectivity and permeability. He found that both selectivity and permeability are inversely related and thus there has to be some trade off when a user wants to use it for commercial purposes. Low selectivity will require large area of membranes and thus large cost. Low permeability will require high amount of time, and to compensate that a user will have to install high number of membrane modules resulting in huge cost. However, after various technological innovations, Robeson again studied these polymers

and found that upper limit for permeability and selectivity has moved slightly to upper right corner [8].

Henis and tripodi prepared a defect free membrane [11] and it consists of a selective layer of rubber on porous support resulting in asymmetric membrane. Top selective layer can be any polymer which has affinity for lower porous base membrane. Selective layer can also incorporate inorganic filler, since it will increase selectivity. Researchers are investigating these membrane materials due to their better performance compared to other materials [12].

Li et al [13] found the effect of polyethylene glycol (PEG) on permeability and selectivity of CA membrane using different molecular weights of PEG. Permeability increase with lower molecular weight PEG-200 but selectivity increases after adding 10% PEG-20000 in CA polymer. Also, this resulted in increase of glass transition temperature of blended polymer from 185.5 C for pure membrane to 197 C for membrane with PEG-20000.

2.3. Facilitated Transport Membranes

Facilitated Transport Membranes (FTM) are known for their enhanced permeabilities due to carbonate and bicarbonate formation in the presence of water. In industrial application presence of water vapors in gas streams reduces CO₂ permeability. Facilitated transport membranes are different in this respect, they facilitate CO₂ permeation and thus more effective. Kim et. al. [14] demonstrated that in the presence of PVAm membranes CO₂ permeability increases significantly.

2.4. Fixed Site Carrier Membranes

Fixed site carrier membranes (FSC) have been found to have increasing permeability effect for CO₂. This is due to the increased interaction with fixed sites. Deng et. Al. [15] studied crosslinked PVAm FSC membrane. This membrane has amine groups as a carrier site for CO₂. FSC membranes have one serious disadvantage. They tend to lose carrier sites with the passage of time due to degradation. [16]. Facilitated transport membranes and polymeric blends have low tolerance for CO₂ plasticization but fixed site carrier membranes are less prone to this effect due to extra free volume created by fixed site carriers.

2.5. Mixed Matrix Membranes (MMM)

Mixed Matrix Membranes (MMM) is a major leap forward in gas separation. In MMM, different organic/inorganic fillers are incorporated within polymers to modify their properties. Fillers include ZIFs, Metal Organic frameworks (MOF), CNTs, TiO₂.

S. Farrukh et. al. [11] studied the behavior of gas permeability and selectivity with the addition of TiO₂. Permeability of carbon dioxide was increased due to interaction between CO₂ and TiO₂ nanoparticles having size of 5 – 10 nm. Cornelius et al. [17] showed the permeability behavior of polyimide having embedded silica with the addition of different alkoxyselanes. Thermal treatment of membrane resulted in enhanced permeability with no change in selectivity.

A. L. Khan et al. [18] demonstrated that how counter-ion alter the permeation of mixed gases through sulfonated poly (ether ether ketone) (S-PEEK). CO₂/CH₄ selectivity was decreased owing to the increase in permeability of both CO₂ and CH₄ due to change in mobility of polymer chains. These membranes have shown selectivity of maximum of 18.60.

Mixed Matrix Membranes (MMM) are superior to other membranes due to its molecular sieving ability, enhance tensile strength, adsorption at the surface and availability of extra path through fillers. CNTs are one of the contender, having great CO₂ adsorption of 22.7 mg/g.

M. M. Khan et al. [19] studied the permeation behavior of gases with the addition of CNTs. Addition of PEG along with CNTs increased interaction and enhanced both permeability of carbon dioxide and selectivity of CO₂/CH₄ attained is 16.3. Liyuan et al. [15] investigated effect of PVAm/PVA blended membranes on separation of carbon dioxide from methane. Permeance increased by 0.35 m³(STO)/m².h and selectivity of 45 was reported.

A. R. Moghadassi et al [9] showed that enhanced mechanical strength was achieved with the synthesis of cellulose Acetate (CA) based (MMM) using MWCNTs as fillers. CO₂/CH₄ selectivity changed from 13.41 to 21.81. selectivity of 53.98 was observed at 2 bar.

2.6. Objective

It has been shown that CNTs have better CO₂ adsorption capacity and are therefore suitable choice as a filler. MWCNTs incorporation into different polymers need to be investigated to better understand the contribution of polymer in CO₂ permeability and CO₂/CH₄ selectivity. It will also verify the CNTs behavior demonstrated by the above-mentioned authors.

In this study, Polyamide 6 (PA6) is taken as a base polymer. Due to relatively high temperature requirement for the synthesis of PA 6 based membranes, Polyethylene glycol was not added as a binder in these membranes. PEG decompose at around 44 C. MWCNTs were added in different weight percentages in PA6 membranes to study the effect of CNTs in CO₂ permeability and CO₂/CH₄ selectivity.

Chapter – 3

Experimental Methods

3.1. Materials

Following materials have been used:

- I. Polyamide 6 (MW 339), purchased from Sigma Aldrich
- II. Formic Acid (98% purity), purchased from Sigma Aldrich.
- III. Phenol (98% purity), purchased from Fischer.
- IV. Multi-walled carbon nanotubes (MWCNTs) with purity: > 95%; OD: 8 – 15 nm; ID: 3-5 nm, were bought from Yurui Shanghai Chemical.
- V. The CO₂ and CH₄ was purchased from Linde Pakistan.

3.2. Solution Preparation

Pure PA membranes were fabricated by using solution casting method. The PA membranes were dissolved in Formic Acid in different weight percent. The thickness appropriate for gas separation is 25 – 30 nm. It is obtained by adding 0.16 g PA in 7.84 g Formic Acid. The solution was stirred in sealed glass bottles for 24 hours. After that it is poured on petri dish and placed in oven. Pure polymeric membranes were prepared in oven at 65 °C, 70 °C, 75 °C, 80 °C. Different weight fractions of MWCNTs were added in Formic Acid and mixed for 30 mins at room temperature to make homogeneous mixture. After that solutions were sonicated using ultrasonic mixer (Vibra-Cell VC130, Sonics & Materials, Inc.) using a 5 s pulse and 60% amplitude. Solution was then sonicated with a 10 s pulse and 20% amplitude for 30 mins. This is added to pre-stirred solution of PA in Formic Acid and stirred for 24 h. After that final solutions were sonicated again for 30 mins at 10% amplitude and 10 s pulse. These solutions were then poured in petri dishes at elevated temperature of 70 °C for 2 hrs. Eight different concentrations of MWCNTs (8,9,10,11,12,13,14,15 wt.%) were added in PA.

3.3. Membrane Casting

Prepared solution having low viscosity were poured in petri dishes are placed in oven at different temperatures for 2hrs. thickness of membranes were below $30\mu\text{m}$ for pure PA6 but above $35\mu\text{m}$ for MWCNTs/PA6 based MMM membranes.

3.4. Permeation Testing Apparatus

3.4.1. Equipment Description

Permeation of CO_2 and CH_4 is measured as single gas using the Gas permeability test system from (PHILOS, Korea).

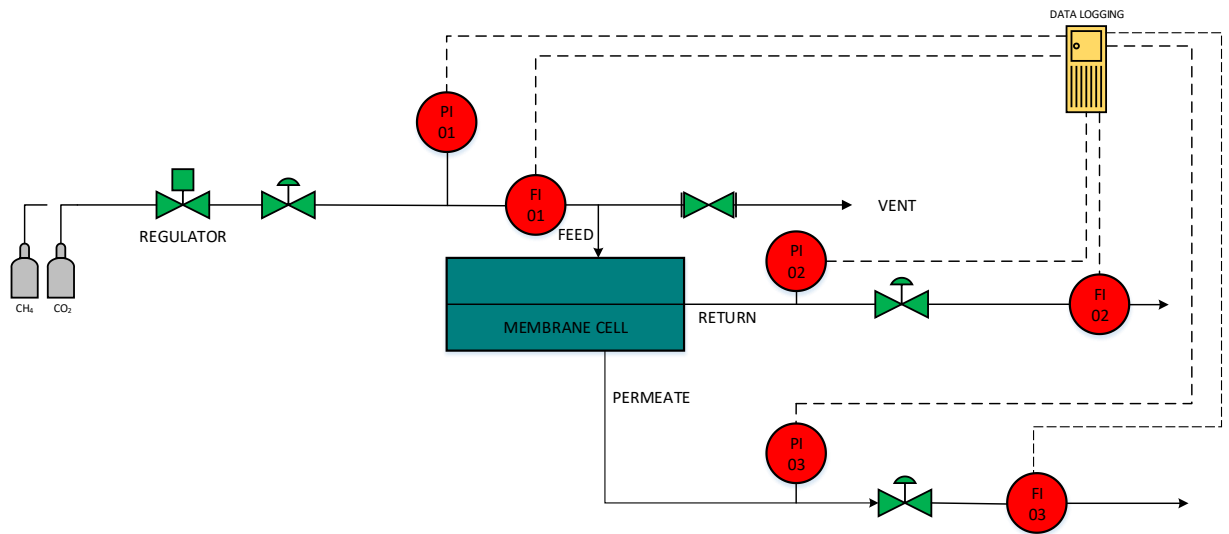


Figure 11: Gas Permeability Test System

This system has support disk with an effective area of 8.5 cm^2 and is made of ceramic. Bubble flow meter has been utilized to measure flow rate of gases below 10 ml/s . permeability test system provides us flowrate at every pressure difference value from which permeability can be calculated.

3.4.2. Instrumentation

Gas permeability test system contains following instrumentation

- I. Back pressure valve
- II. Mass flow controllers
- III. Flow indicators

- IV. Bubble flow meter
- V. Pressure indicators

3.4.3. Working of Gas Permeability Test system

Permeation of samples were performed using permeation testing apparatus from Malaysia (Fig. 11). Permeation testing apparatus includes gas cylinder, membrane module, pressure regulators, Valve, Flow meter. Membrane module was made of stainless steel and consists of high pressure and low pressure compartments and membrane is placed in between. The effective membrane area was 8.5 cm². Gas is charged from high pressure compartment to membrane. High pressure was supplied from gas cylinder. Pressure on feed side varied from 0.5 to 5 bar. Pressure on permeate side was atmospheric pressure (1 bar). Pressure was adjusted at feed side using regulators. Permeation behavior was recorded for methane and carbon dioxide. First permeation testing was performed for CH₄ than for CO₂ because it can cause plasticization of PA membranes. Cross sectional area of 8.5 cm² was placed in membrane module. Permeability of both gases was calculated using the following equation: [9].

$$P = \frac{QL}{\Delta PA}$$

where A is an effective membrane area (m²), Q is volumetric gas flow rate (ml/min), L is the thickness of membrane (m) and pressure difference is ΔP (bar). P is permeability of gas in barrer.

Selectivity of membrane (α_{CO_2/CH_4}) is determined by formula: [10]

$$\alpha_{CO_2/CH_4} = \frac{P_{CO_2}}{P_{CH_4}}$$

where P_{CO₂} and P_{CH₄} are permeabilities of CO₂ and CH₄ respectively.

Chapter – 4

Resources and Approaches

4.1. Characterization Techniques

4.1.1. Scanning Electron Microscopy (SEM):

To analyze structure and morphology of membrane at nanometers level Scanning electron microscopy is needed. High energy electrons are bombarded on the surface of material. SEM is used to determine the surface and cross section of membranes. Membranes were coated with gold and analyzed at 10 mm distance and with current of 90 mA.

Scanning electron microscope (SEM) is used to analyze the structure and morphology of membranes. High energy electrons are focused on the surface of the material. The analysis is performed to determine the surface and cross sectional morphology. Membranes were prepared by sputter coating of gold and analyzed at 10mm distance and 90mA current in SEM.

4.1.1.1. Components of SEM

SEM has following components

- I. Display
- II. Vacuum system
- III. Detector
- IV. Scanning system
- V. Electron column
- VI. Electronic control

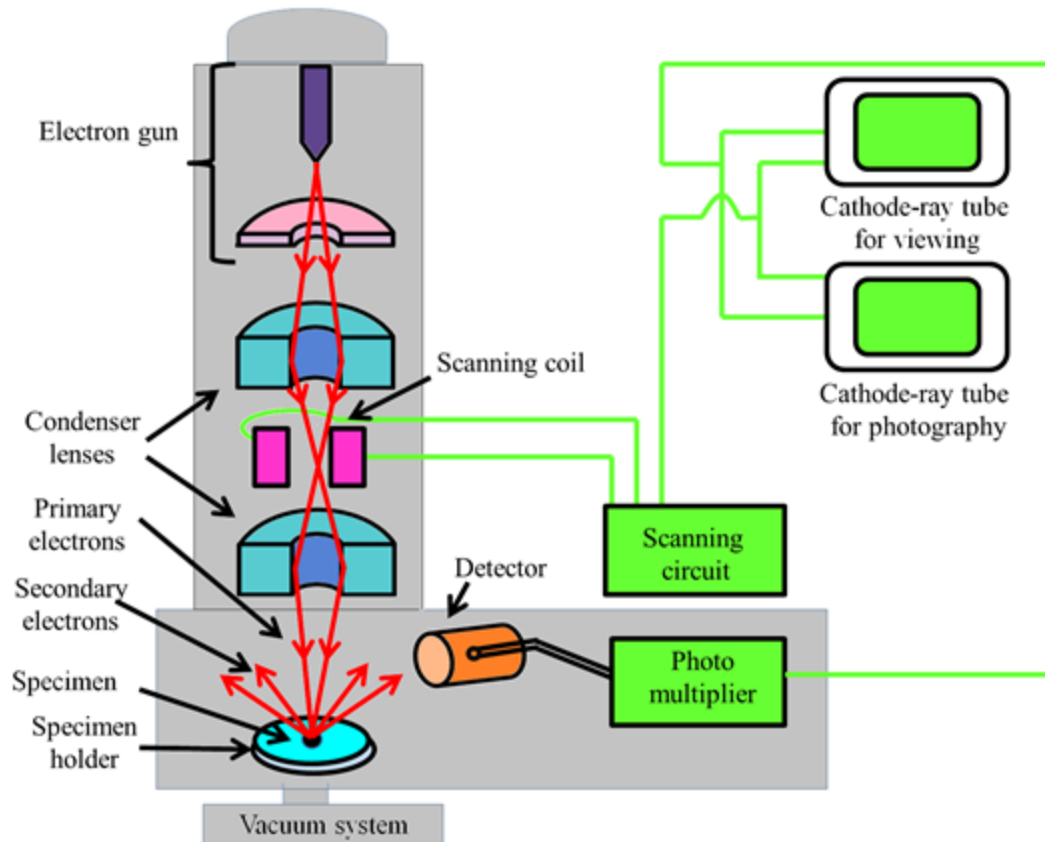


Figure 12: Schematics of scanning electron Microscope

4.1.1.2. Working principle

High energy electrons are focused on the surface of material. For image of material secondary electrons are used while backscattered electrons are used for phase determination. The secondary electrons show the morphology and topology of membrane material. SEM is usually nondestructive technique because at lower magnification sample does not damage.

4.1.1.3. Magnification in SEM:

SEM uses electrons to show the image instead of optics. By tuning the length of scan (L_{spec}) on material we can adjust magnification. Calibration is important for every equipment and for SEM calibration is necessary. Length of scan of monitor is constant (L_{mon}), and thus linear magnification can be determined from the following formula:

$$M = \frac{L_{mon}}{L_{spec}}$$

4.1.1.4. Quality of the Image

Image formation in SEM depends upon detector. Signal (S) is measured by counting electrons falling on detector. The noise (N) reduces the signal and quality is diminished. By increasing number of counts, quality can be improved since it is ratio of signal to noise (S/N).

Contrast is defined as:

$$C = \frac{S_2 - S_1}{S_2}$$

4.1.1.5. Image formation

SEM forms an intensity map which is two dimensional. Each pixel is indicative of a point on sample which is related to the intensity of sample.

SEM forms a two-dimensional intensity map and each pixel on the map is representative of a point of the sample which is directly related to the intensity of the signal (Fig. 12). It is not possible for SEM to generate a true image rather the image is displayed electronically. SEM determines two characteristic features of a material: Morphology, Topography

4.1.2. Thermal Gravimetric Analysis (TGA)

TGA is used to investigate weight change and thermal stability of a material. Weight change depends on temperature and time at constant temperature. The inert atmosphere is provided usually of nitrogen. TGA can be used for analysis of metals, composites, polymers. Analysis was done under rate of heating of 10 °C/min while nitrogen gas flow was maintained at 80 ml/min and temperature variation was from 40 to 700 °C [20].

4.1.2.1. Instrumentation

TGA schematics is shown below:

instrumentation

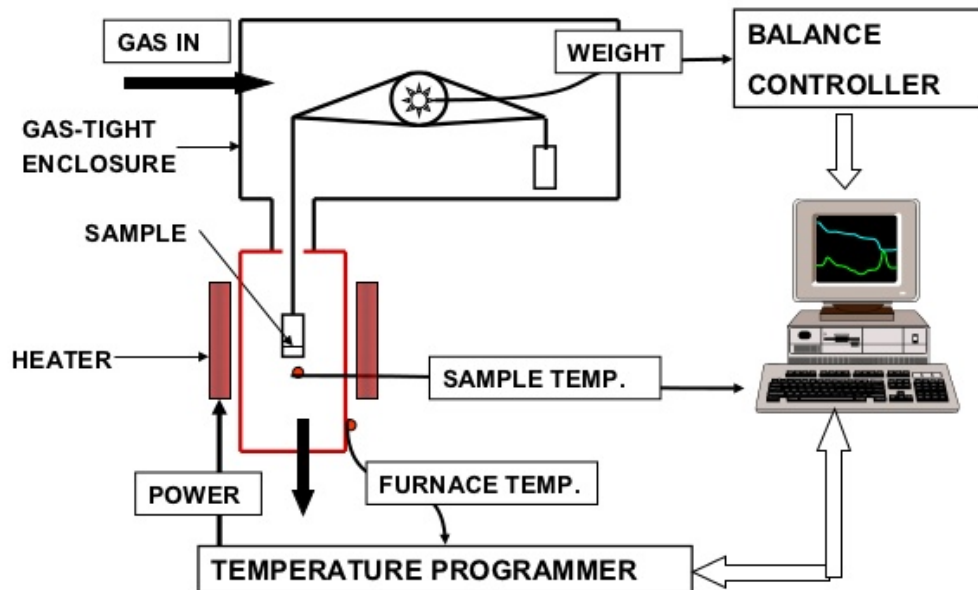


Figure 13: Schematics of Thermal Gravimetric Analysis

It consists of following components

- I. Sample changer
- II. Furnace
- III. IR detector
- IV. Electronic microbalance
- V. Optical filter

Sample changer is a plate in which specified weight of sample is placed. Furnace is the main heat source, which provide heat to the sample and it results in reduction of its weight. IR detector is infrared detector. Heat is usually detected by infrared radiation and here IR detector determines the amount of heat being provided to the sample. Electronic microbalance is used for weight measurement. Since by applying heat weight of sample is reduced therefore to measure the continuously reduced weight we need electronic microbalance. Optical filter filters the light coming out of the sample.

4.1.2.2. Working principle

TGA has sample holder in the form of pan where samples are placed to be analyzed. The pan is heated using furnace throughout the experiment. Changes in weight of initial sample is recorded with respect to temperature. Inert atmosphere of nitrogen is provided. Through this procedure thermal stability is determined.

4.1.2.3. Types of thermogravimetry

- I. **Isothermal TGA:** At constant temperature, sample is heated for fixed period of time and weight change is determined
- II. **Dynamic TGA:** At constant heating rate, change in sample of weight is determined
- III. **Quasi-static TGA:** At constant heating rate but with variation in temperature, change in sample weight is determined.

4.1.2.4. Factors affecting TGA curve

TGA curve is dependent on the following factors

- I. Heating rate
- II. Sample size
- III. Packing
- IV. Crucible shape
- V. Gas flow (N₂ flow in this case)

4.1.2.5. Information obtained from TGA

TGA show the following information about our samples.

- I. Sample decomposition temperature
- II. Thermal stability
- III. Kinetic parameters related to reactions that might occur in samples

4.1.3. Mechanical Testing

Tensile testing is characterization technique to determine the mechanical stability of material. In this test material undergoes through stress and the resulting deformation produced from stress is measured. The tensile testing is used to measure the stress-strain curve. Material is taken in standard length and area. The standard length is known as gauge

length. Stress is induced in a material at constant rate and strain is recorded. Stress and strain is defined by the following equations:

$$\text{Stress} = \frac{\text{Force}}{\text{Area}}$$

$$\text{Strain} = \frac{\text{Change in length}}{\text{Original length}}$$

Mechanical testing is usually done to get a knowledge about material properties like elasticity, toughness, ductility, and resilience.

4.1.3.1. Universal Testing Machine (UTM)

UTM is used for mechanical testing of material. It consists of the following parts.

- I. Frame
- II. Engine
- III. Gear
- IV. Screws
- V. Crosshead
- VI. Gripping Jaws
- VII. Extensometer
- VIII. Specimen
- IX. Hardware and Software Control

4.1.3.2. Working principle

The specimen to be tested is placed between jaws of UTM and force in axial direction is applied while recording the resulting strain through computer software. Strain recording is done until material fracture. Relationship between stress and strain is determined through change in length.



Figure 14: Universal Testing Machine (UTM)

4.1.4. X-ray Diffraction (XRD)

XRD analysis is performed to determine the crystallinity of material. XRD shows a researcher that how the atoms are packed in material, bond length and angles.

4.1.4.1. Instrumentation

Figure below shows the schematics of X-ray Diffractometer

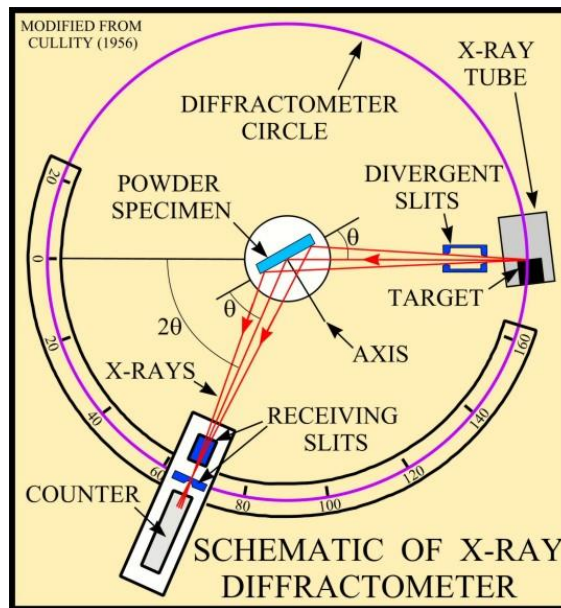


Figure 15: X-Ray Diffractometer Schematics

It has following main components:

- I. X-ray Source
- II. Monochromator
- III. Goniometer
- IV. Detector

4.1.4.2. Working principle

Working principle of XRD depends upon inference of monochromatic ray. X-rays are made to fall on the sample placed on monochromator. Every material has different atomic arrangements which depends upon whether a material is crystalline or amorphous. X-rays after striking the specimen reflects and strikes detector. Two phenomena occur in this process, refraction and diffraction. Diffracted rays are absorbed in the material. The diffraction of light varies from material to material and is highly dependent of arrangement of atoms within crystal lattice. Difference between atoms within lattice is measured by Bragg's law:

$$n\lambda = 2d \sin\theta$$

n = order of diffracted beam

λ = wavelength of incident x-ray beam

d = distance between adjacent planes of atoms

Material can be easily determined by matching XRD curve with reference pattern

4.1.4.3. Applications

X-ray diffraction analysis is widely used for following applications

- I. To identify unknown crystalline material
- II. To Determine unit cell dimensions
- III. To check the purity of sample

Chapter – 5

Results and Discussions

5.1. Scanning Electron Microscopy (SEM)

Scanning electron microscope was used for analyzing the surface and cross section of membrane. Surface morphology of membranes were studied by using Scanning Electron microscope (SEM). Surface and cross section of pure Polyamide 6 membranes at 80 °C is shown in Fig. 16 (a) & (b). SEM imaging shows that Nylon 6 membrane is dense at 80 °C. This also shows the smooth surface of pure PA6 membrane. Fig 16 (c) & (d) shows surface and cross section 10wt% MWCNTs/PA 6 and it shows the void creation at thickness of under 30 μm . Fig 16 (e) & (f) shows the SEM imaging of 10wt% MWCNTs/PA-6 above thickness of 50 μm which shows that increasing thickness reduces probability of void creation in membranes. Also this shows the effective bonding between polymer particles and filler. Figure 16 (c), (d), (e), (f) shows granules which indicates the homogeneous mixing of Carbon nanotubes in polymer matrix. Scanning Electron microscopy indicates that nano particles are homogeneously distributed in polymer matrix. Voids creation in low thickness membrane due to CNTs is due to agglomeration of Carbon nanotubes [21]. Also with thin membrane, its ability to withstand stress reduces and thus nanoparticles create voids in membranes. Fig 16 (b) shows that processing path taken to prepare nano composites may result in agglomeration of CNTs and caused large scale voids in polymer matrix. This results in low resistance pathway for the passage of gas. In such case diffusion becomes Knudsen diffusion.

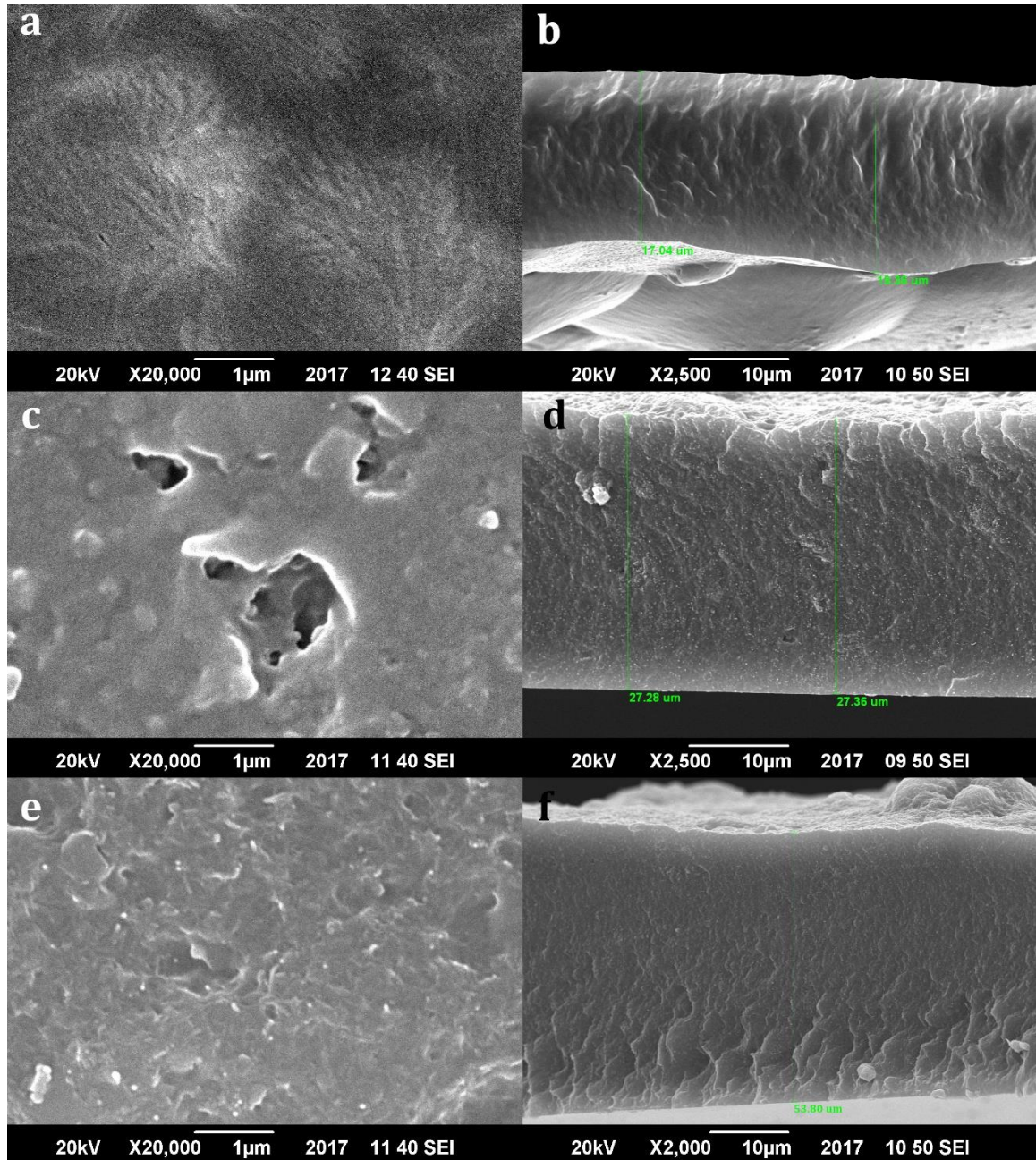


Figure 16: Surface Morphology and Cross section
a pure membrane, *c* 10wt% CNTs under 30 μm , *e* 10wt% CNTs above 50 μm (Surface Morphology)
b pure membrane, *d* 10wt% CNTs under 30 μm , *f* 10wt% CNTs above 50 μm (Cross Section)

5.2. Gas Permeation Study

Gas permeation was performed on testing apparatus illustrated in Fig. 11 [8]. The membranes synthesized from solution casting method were cut in circular shape of 3.28 cm diameter and placed in a membrane cell.

5.2.1. Thickness Adjustment of membranes

First of membrane thickness has to be adjusted to below 30 μm since all industrial membranes use membranes of thickness between 25 μm – 30 μm .

Table 2: Pure PA 6 membranes of different thickness

Membrane	Membrane Material	Solvent	Polymer wt%
M1	Pure Nylon, 6	Formic Acid	14
M2	Pure Nylon, 6	Formic Acid	10
M3	Pure Nylon, 6	Formic Acid	8
M4	Pure Nylon, 6	Formic Acid	5
M5	Pure Nylon, 6	Formic Acid	3
M6	Pure Nylon, 6	Formic Acid	2

Membrane required for commercial application need to have thickness below 30 μm . Therefore, first thickness was adjusted. First of all, 1.12 g of PA6 was added into 6.88 g of formic Acid. It resulted in 132 μm of thickness. After that 0.8 g of PA6 was added to 7.2 g of formic Acid. This resulted in thickness of 97 μm . Then 0.64 g of PA6 was added to 7.36 g of formic Acid. It resulted in thickness of 79 μm . Further thickness has to be reduced and for this purpose 0.4 g of PA6 was added to 7.6 g of formic Acid and casted on petri dish. This resulted in 53 μm of thickness. After that 0.24 g of PA6 was added to 7.76 g of formic Acid. This resulted in slightly high thickness of 36 μm . So further thickness was reduced by taking 0.16 g of PA6 in formic acid. This resulted is desirable thickness of 27.3

μm . The membrane **M6** has thickness of around **27.3 μm** and is desirable since it can be used as an industrial membrane.

5.2.2. Addition of MWCNTs in PA6 Membrane in Formic Acid

Multi walled Carbon Nanotubes were added in Formic Acid and sonicated for specified period of time. After that it is mixed in another solution of PA6 in Formic Acid.

Table 3: MWCNTs in PA6 with different wt % of PA6 in Formic Acid

Membrane	Membrane Material	Polymer wt%
M7	15 wt% MWCNTs / Nylon, 6	2
M8	10 wt% MWCNTs / Nylon, 6	3
M9	10 wt% MWCNTs / Nylon, 6	2.22
M10	10 wt% MWCNTs / Nylon, 6	2.5
M11	1 wt% MWCNTs / Nylon, 6	3
M12	3 wt% MWCNTs / Nylon, 6	3
M13	5 wt% MWCNTs / Nylon, 6	3
M14	7 wt% MWCNTs / Nylon, 6	3
M15	8 wt% MWCNTs / Nylon, 6	3
M16	9 wt% MWCNTs / Nylon, 6	3
M17	11 wt% MWCNTs / Nylon, 6	3
M18	12 wt% MWCNTs / Nylon, 6	3
M19	13 wt% MWCNTs / Nylon, 6	3
M20	14 wt% MWCNTs / Nylon, 6	3

Addition of fillers were done in 3 wt % thickness of membranes. since 2 wt % polymer is only suitable for pure PA6 membrane. Addition of MWCNTs in 2 wt % polymer creates voids so large that they can be seen from naked eye. After that different weight percentages of fillers were added in polymer. Weight percent of filler below 8 wt % does not disperse

homogeneously and has shown parallel lines of fillers due to shrinkage effect. Therefore, fillers of 8 wt % or above are suitable for study.

5.2.2.1. Results

5.2.2.1.1. Permeabilities of pure PA6 membrane

Permeabilities of pure PA6 membrane were calculated at different temperatures. The temperatures selected were 65 °C, 70 °C, 75 °C, 80 °C

Table 4: Permeabilities of CO₂ and CH₄ at different Temperatures

T	pCO ₂ (Sample 1)	pCO ₂ (Sample 2)	pCO ₂ (Sample 3)	pCH ₄ (Sample 1)	pCH ₄ (Sample 2)	pCH ₄ (Sample 3)
65.00	2,572.81	2,591.31	2,754.25	4,440.86	4,482.31	4,678.61
70.00	9,302.81	9,386.12	9,459.20	13,886.91	13,898.90	14,367.54
75.00	13,816.00	13,756.45	14,539.23	19,658.00	19,669.23	20,891.57
80.00	16,098.86	16,043.23	17,548.95	21,786.86	21,795.26	23,387.26

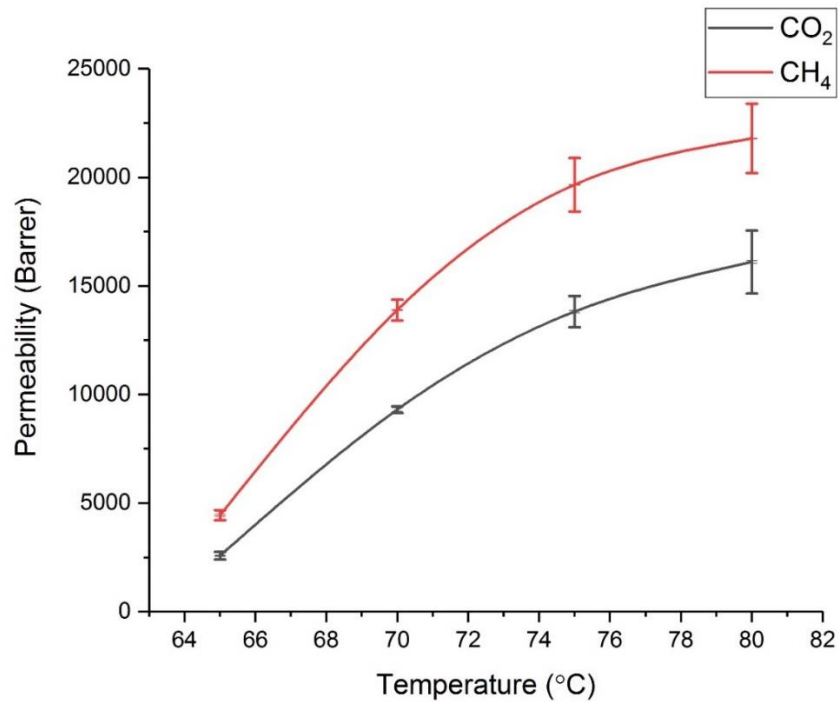


Figure 17: Permeabilities of CO₂ and CH₄ at different Temperatures

As can be seen from the above graph that with increasing temperature, permeability of both gases (i.e. CO₂ and CH₄) increases. Permeabilities of CH₄ are greater than CO₂ because of high sorption coefficient of CH₄ compared to that of CO₂. Since gases have high flow rate, sorption phenomena is dominant compared to diffusion. At 65 °C, CH₄ has permeability of 4534 barrer whereas CO₂ permeability is 2639 barrer. This shows that CO₂ permeability is considerably lower than that of CH₄. However, the trend remains same as temperature is increased. With increasing temperature, permeability increases for both gases. At maximum temperature of casting (i.e. 80 °C), CH₄ permeability increased to 22,324 barrer while CO₂ permeability increased to 16564 barrer. Since the membrane has low gas selectivity, it is desirable to cast this membrane at high temperature because this results in high permeabilities.

5.2.2.1.2. Permeabilities of MWCNTs/PA6 membranes in Formic Acid

Following are the permeabilities of CO₂ and CH₄ observed. Very high permeabilities are not measurable.

Table 5: Permeabilities of MWCNTs/PA6 membranes in Formic Acid

MWCNTs Weight %	Permeability (CO₂)	Permeability (CH₄)
8.00	Very High	Very High
9.00	Very High	Very High
10.00	73.56	136.65
11.00	Very High	Very High
12.00	11,588.12	17,817.47
13.00	243.00	647.00
14.00	3,989.00	5,378.00
15.00	Very High	Very High

Table 5 indicates that permeabilities of gases through membranes are very high in case of Mixed Matrix Membranes. At 8,9,11,15 wt% of MWCNTs in PA6, membranes synthesized were defective and had voids. The voids were observable in SEM and resulted in permeabilities so high which cannot be measured. However, membrane synthesized at 10, 12, 13, 14 wt% were defect free and resulted in relatively lower permeabilities.

Permeabilities observed at 12 wt% were highest for both gases where as it is lowest for 10 wt% of carbon nanotube filler. The trend is irregular and therefore does not led to any conclusion.

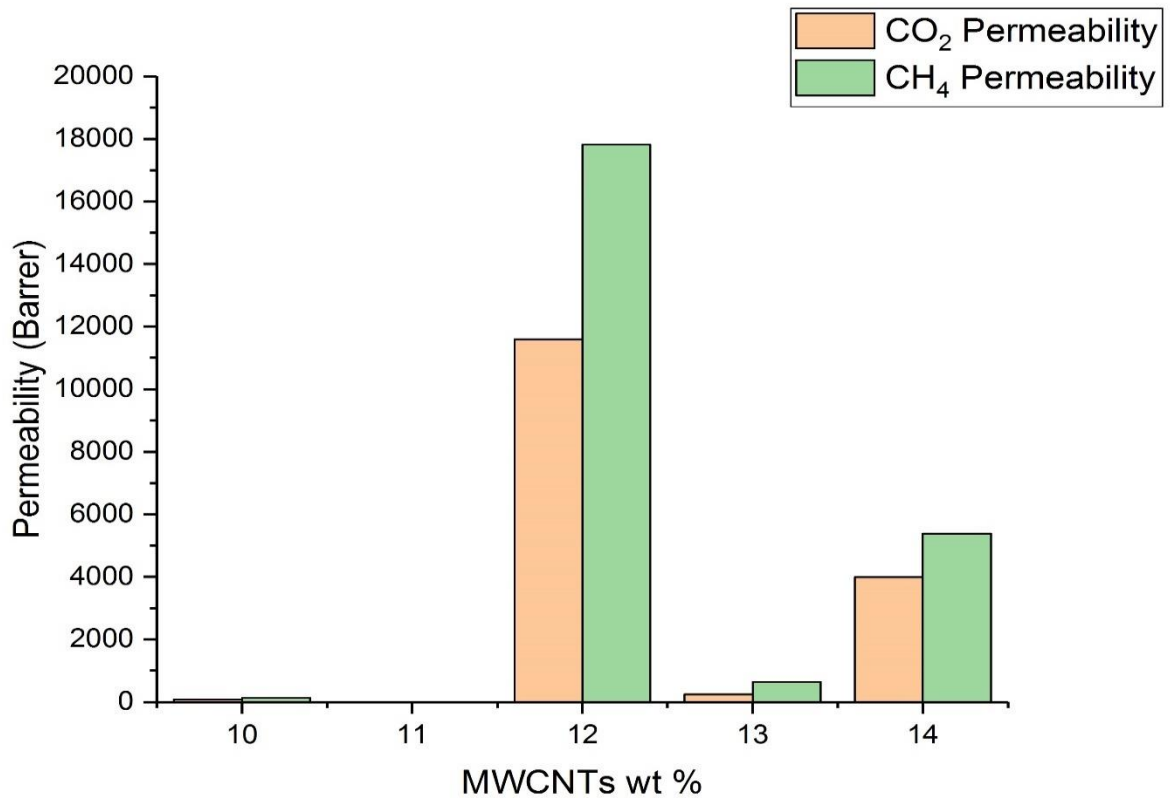


Figure 18: Permeabilities of MWCNTs/PA6 membranes in Formic Acid

As can be seen that permeabilities are so high for all CNTs wt% except for 10 wt% of CNTs. This trend is irregular and is indicative of some defect in membranes. Scanning electron microscopy has revealed that membranes have void which were created due to low thickness of base polymer PA6. Therefore, addition of MWCNTs require high thickness of membranes.

Figure 18 indicates that permeabilities of gases through membranes are very high in case of Mixed Matrix Membranes. At 8,9,11,15 wt% of MWCNTs in PA6, membranes synthesized were defective and had voids. The voids were observable in SEM and resulted

in permeabilities so high which cannot be measured. However, membrane synthesized at 10, 12, 13, 14 wt% were defect free and resulted in relatively lower permeabilities. Permeabilities observed at 12 wt% were highest for both gases where as it is lowest for 10 wt% of carbon nanotube filler. The trend is irregular and therefore does not led to any conclusion.

5.2.2.1.3. Selectivities of MWCNTs/PA6 membranes in Formic Acid

Table 6: Selectivities of MWCNTs/PA6 membranes in Formic Acid

MWCNTs Weight %	α CO ₂ /CH ₄	α CH ₄ /CO ₂
8.00	-	-
9.00	-	-
10.00	0.54	1.86
11.00	-	-
12.00	0.65	1.54
13.00	0.38	2.65
14.00	0.74	1.35
15.00	-	-

(-) sign indicates that selectivities are not measurable.

Since selectivities are dependent on permeabilities, the trend is random same as for permeabilities, as can be seen from above Table. Also, this shows that at 10, 12, 13, 14 wt % where permeabilities are relatively measurable, selectivities are not sufficient to constitute efficient separation. This trend is irregular and is indicative of some defect in membranes. Scanning electron microscopy has revealed that membranes have void which were created due to low thickness of base polymer PA6. Therefore, addition of MWCNTs require high thickness of membranes.

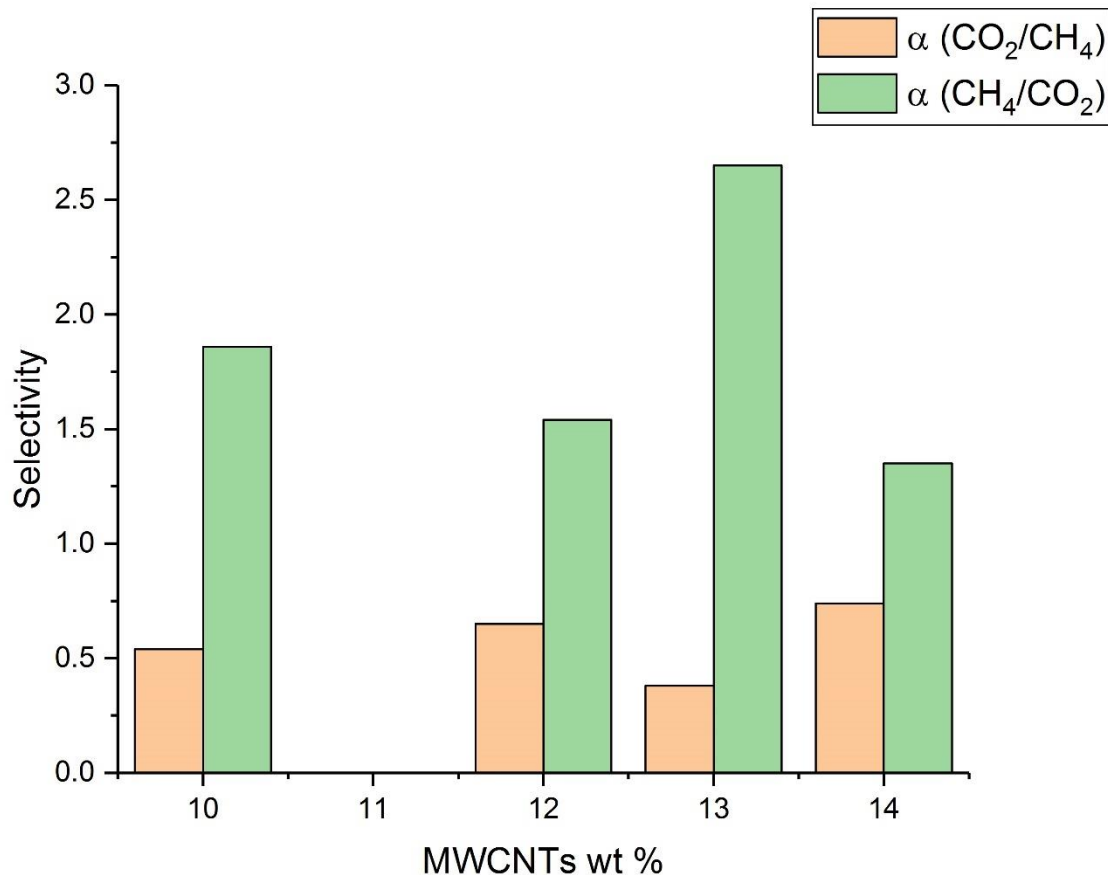


Figure 19: Selectivities of MWCNTs/PA6 membranes in Formic Acid

Fig. 19 indicates selectivity of membranes with fillers v/s filler wt%. as can be seen in above table that due to non-repeatability of experiments the data obtained is irregular and in some cases due to void formation, permeability is so high that it becomes practically unmeasurable. Since selectivities are dependent on permeabilities, the trend is random same as for permeabilities, as can be seen from above graph. Also, this shows that at 10, 12, 13, 14 wt % where permeabilities are relatively measurable, selectivities are not sufficient to constitute efficient separation. This trend is irregular and is indicative of some defect in membranes. Scanning electron microscopy has revealed that membranes have void which were created due to low thickness of base polymer PA6. Therefore, addition of MWCNTs require high thickness of membranes.

5.2.2.1.4. Permeabilities of MWCNTs/PA6 membranes in Formic Acid

Here again samples were made to check the reproducibility of samples.

Table 7: Permeabilities of MWCNTs/PA6 membranes in Formic Acid

Weight %	Permeability (CO ₂)	Permeability (CH ₄)
8.00	Very High	Very High
9.00	Very High	Very High
10.00	560.43	980.31
11.00	Very High	Very High
12.00	Very High	Very High
13.00	9,834.76	13,034.68
14.00	4,618.32	6,262.04
15.00	5,215.21	9,042.87

Table 7 indicates that permeabilities of gases through membranes are very high in case of Mixed Matrix Membranes. At 8, 9, 11, 12 wt% of MWCNTs in PA6, membranes synthesized were defective and had voids. The voids were observable in SEM and resulted in permeabilities so high which cannot be measured. However, membrane synthesized at 10, 13, 14, 15 wt% were defect free and resulted in relatively lower permeabilities. Permeabilities observed at 13 wt% were highest for both gases where as it is lowest for 10 wt% of carbon nanotube filler. The trend is irregular and therefore does not led to any conclusion.

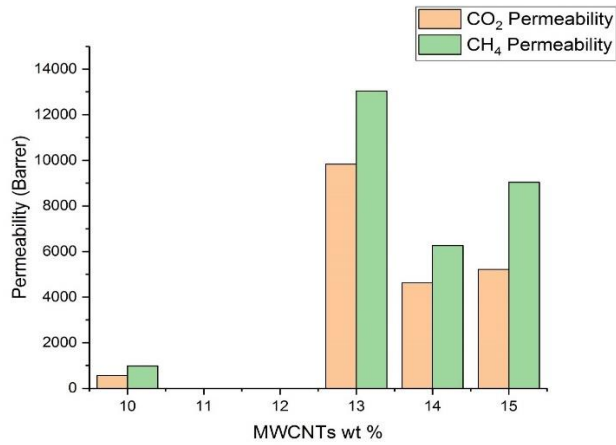


Figure 20: Permeabilities of MWCNTs/PA6 membranes in Formic Acid

As shown in above bar graph that trend for permeabilities are once again random, far from desirable behavior.

As can be seen that permeabilities are so high for all CNTs wt% except for 10 wt% of CNTs. This trend is irregular and is indicative of some defect in membranes. Scanning electron microscopy has revealed that membranes have void which were created due to low thickness of base polymer PA6. Therefore, addition of MWCNTs require high thickness of membranes.

Figure 20 indicates that permeabilities of gases through membranes are very high in case of Mixed Matrix Membranes. At 8, 9, 11, 12 wt% of MWCNTs in PA6, membranes synthesized were defective and had voids. The voids were observable in SEM and resulted in permeabilities so high which cannot be measured. However, membrane synthesized at 10, 13, 14, 15 wt% were defect free and resulted in relatively lower permeabilities. Permeabilities observed at 13 wt% were highest for both gases where as it is lowest for 10 wt% of carbon nanotube filler. The trend is irregular and therefore does not led to any conclusion.

5.2.2.1.5. Selectivities of MWCNTs/PA6 membranes in Formic Acid

Table 8: Selectivities of MWCNTs/PA6 membranes in Formic Acid

Weight %	α CO ₂ /CH ₄	α CH ₄ /CO ₂
8.00	-	-
9.00	-	-
10.00	0.57	1.75
11.00	-	-
12.00	-	-
13.00	0.75	1.33
14.00	0.74	1.36
15.00	0.58	1.73

Table 8 indicates selectivity of membranes with fillers v/s filler wt% as can be seen in above table that due to non-repeatability of experiments the data obtained is irregular and

in some cases due to void formation, permeability is so high that it becomes practically unmeasurable. Since selectivities are dependent on permeabilities, the trend is random same as for permeabilities, as can be seen from above table. Also, this shows that at 10, 13, 14, 15 wt % where permeabilities are relatively measurable, selectivities are not sufficient to constitute efficient separation. This trend is irregular and is indicative of some defect in membranes. Scanning electron microscopy has revealed that membranes have void which were created due to low thickness of base polymer PA6. Therefore, addition of MWCNTs require high thickness of membranes.

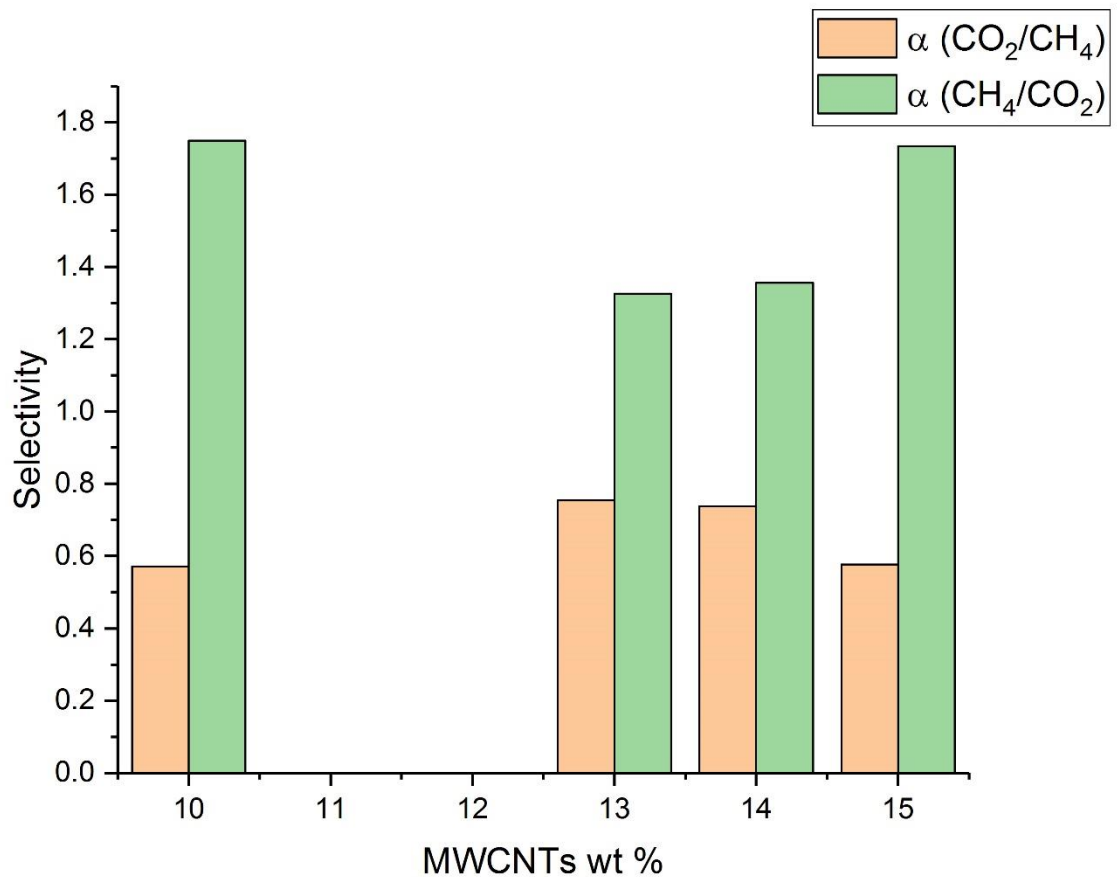


Figure 21: Selectivities of MWCNTs/PA6 membranes in Formic Acid

Selectivities of membranes for the purpose of reproducibility have shown the same irregular trend and are very low. Fig 21 indicates selectivity of membranes with fillers v/s filler wt% as can be seen in above table that due to non-repeatability of experiments the data obtained is irregular and in some cases due to void formation, permeability is so high that it becomes

practically unmeasurable. Since selectivities are dependent on permeabilities, the trend is random same as for permeabilities, as can be seen from above figure. Also, this shows that at 10, 13, 14, 15 wt % where permeabilities are relatively measurable, selectivities are not sufficient to constitute efficient separation. This trend is irregular and is indicative of some defect in membranes. Scanning electron microscopy has revealed that membranes have void which were created due to low thickness of base polymer PA6. Therefore, addition of MWCNTs require high thickness of membranes.

5.2.3. Addition of MWCNTs in PA6 Membrane in Phenol

Since phenol can also dissolve polymer PA6, it was used to check the dispersion of CNTs. Following are the compositions of MMM produced in Phenol. The fillers are added in 3 wt% polymer.

Table 9: MWCNTs in PA6 with different wt % of PA6 in Phenol

Membrane	Membrane Material
M21	8 wt% MWCNTs / Nylon, 6
M22	9 wt% MWCNTs / Nylon, 6
M23	10 wt% MWCNTs / Nylon, 6
M24	11 wt% MWCNTs / Nylon, 6
M25	12 wt% MWCNTs / Nylon, 6
M26	13 wt% MWCNTs / Nylon, 6
M27	14 wt% MWCNTs / Nylon, 6
M28	15 wt% MWCNTs / Nylon, 6

5.2.3.1.Results

5.2.3.1.1. Permeabilities of MWCNTs/PA6 membranes in Phenol

Following are the permeabilities of CO₂ and CH₄ observed. Very high permeabilities are not measurable.

Table 10: Permeabilities of MWCNTs/PA6 membranes in Phenol

MWCNTs Weight %	Permeability (CO ₂)	Permeability (CH ₄)
8.00	Very High	Very High
9.00	Very High	Very High
10.00	6,166.39	9,327.03
11.00	Very High	Very High
12.00	Very High	Very High
13.00	Very High	Very High
14.00	Very High	Very High
15.00	0.00	0.00

As can be seen that membrane of 10 wt% CNTs is the one where permeabilities can be measured. Otherwise permeabilities are very high to be able to measure them. Also at 15 wt% of CNTs, flow has been effectively blocked. That means that this membrane does not have any voids and this is also irregular. Table 10 indicates that permeabilities of gases through membranes are very high in case of Mixed Matrix Membranes. At 8, 9, 11, 12, 13, 14 wt% of MWCNTs in PA6, membranes synthesized were defective and had voids. The voids were observable in SEM and resulted in permeabilities so high which cannot be measured. However, membrane synthesized at 10, and 15 wt% were defect free and resulted in relatively lower permeabilities. Permeabilities observed at 10 wt% were highest for both gases whereas it is zero for 15 wt% of carbon nanotube filler. The trend is irregular and therefore does not lead to any conclusion.

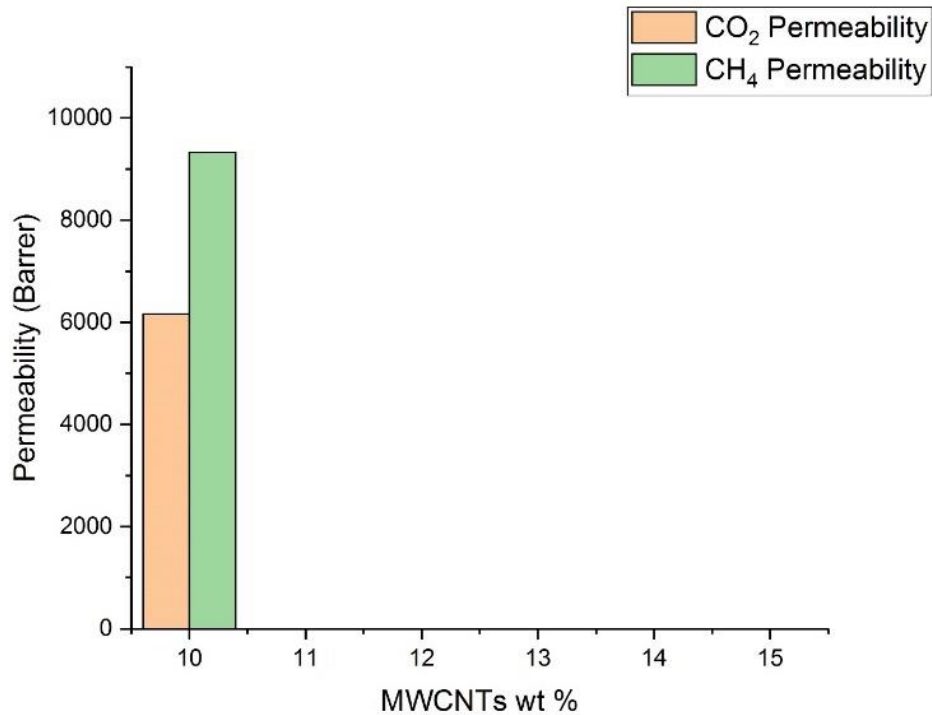


Figure 22: Permeabilities of MWCNTs/PA6 membranes in Phenol

As can be seen that permeabilities are so high for all CNTs wt% except for 15 wt% of CNTs. This trend is irregular and is indicative of some defect in membranes. Scanning electron microscopy has revealed that membranes have voids which were created due to low thickness of base polymer PA6. Therefore, addition of MWCNTs require high thickness of membranes.

Figure 22 indicates that permeabilities of gases through membranes are very high in case of Mixed Matrix Membranes. At 8, 9, 11, 12, 13, 14 wt% of MWCNTs in PA6, membranes synthesized were defective and had voids. The voids were observable in SEM and resulted in permeabilities so high which cannot be measured. However, membrane synthesized at 10, and 15 wt% were defect free and resulted in relatively lower permeabilities. Permeabilities observed at 10 wt% were highest for both gases where as it is zero for 15 wt% of carbon nanotubes filler. The trend is irregular and therefore does not led to any conclusion.

5.2.3.1.2. Selectivities of MWCNTs/PA6 membranes in Phenol

As can be seen from the table below that only 10 wt% CNTs have shown some selectivity but selectivity is too low for industrial application.

(-) sign indicates that selectivities are not measurable.

Table 11: Selectivities of MWCNTs/PA6 membranes in Phenol

MWCNTs Weight %	α CO ₂ /CH ₄	α CH ₄ /CO ₂
8.00	-	-
9.00	-	-
10.00	0.66	1.51
11.00	-	-
12.00	-	-
13.00	-	-
14.00	-	-
15.00	-	-

Since selectivities are dependent on permeabilities, the trend is random same as for permeabilities, as can be seen from above Table. Also, this shows that at 10 wt % where permeabilities are relatively measurable, selectivities are not sufficient to constitute efficient separation. This trend is irregular and is indicative of some defect in membranes. Scanning electron microscopy has revealed that membranes have void which were created due to low thickness of base polymer PA6. Therefore, addition of MWCNTs require high thickness of membranes.

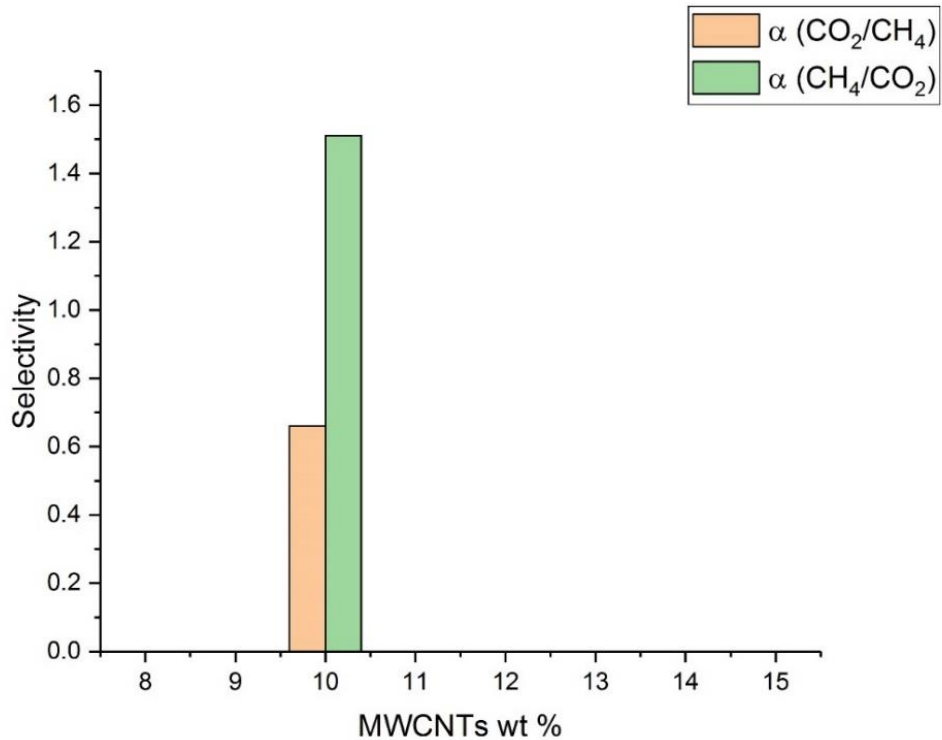


Figure 23: Selectivities of MWCNTs/PA6 membranes in Phenol

Experiments were revised again to check the repeatability of results. Fig. 23 indicates selectivity of membranes with fillers v/s filler wt%. as can be seen in above figure that due to non-repeatability of experiments the data obtained is irregular and in some cases due to void formation, permeability is so high that it becomes practically unmeasurable. Since selectivities are dependent on permeabilities, the trend is irregular, same as for permeabilities, as can be seen from above graph. Also, this shows that at 10 wt % where permeabilities are relatively measurable, selectivities are not sufficient to constitute efficient separation. This trend is irregular and is indicative of some defect in membranes. Scanning electron microscopy has revealed that membranes have void which were created due to low thickness of base polymer PA6. Therefore, addition of MWCNTs require high thickness of membranes.

5.2.3.1.3. Permeabilities of MWCNTs/PA6 membranes in Phenol

Table 12: Permeabilities of MWCNTs/PA6 membranes in Phenol

MWCNTs Weight %	Permeability (CO ₂)	Permeability (CH ₄)
8.00	Very High	Very High
9.00	Very High	Very High
10.00	Very High	Very High
11.00	Very High	Very High
12.00	Very High	Very High
13.00	Very High	Very High
14.00	Very High	Very High
15.00	7,471.96	9,283.09

Now here can be seen that every membrane has pore but 15 wt % CNTs does not have any pore and has measurable permeability. this result is different from the previous one and has shown once again that voids formation is random in MWCNTs/PA6 membranes. Table 12 indicates that permeabilities of gases through membranes are very high in case of Mixed Matrix Membranes. At 8, 9, 10, 11, 12, 13, 14 wt% of MWCNTs in PA6, membranes synthesized were defective and had voids. The voids were observable in SEM and resulted in permeabilities so high which cannot be measured. However, membrane synthesized at 15 wt% were defect free and resulted in relatively lower permeabilities. Permeabilities were observed only at 15 wt% of carbon nanotube filler. The trend is irregular and therefore does not led to any conclusion.

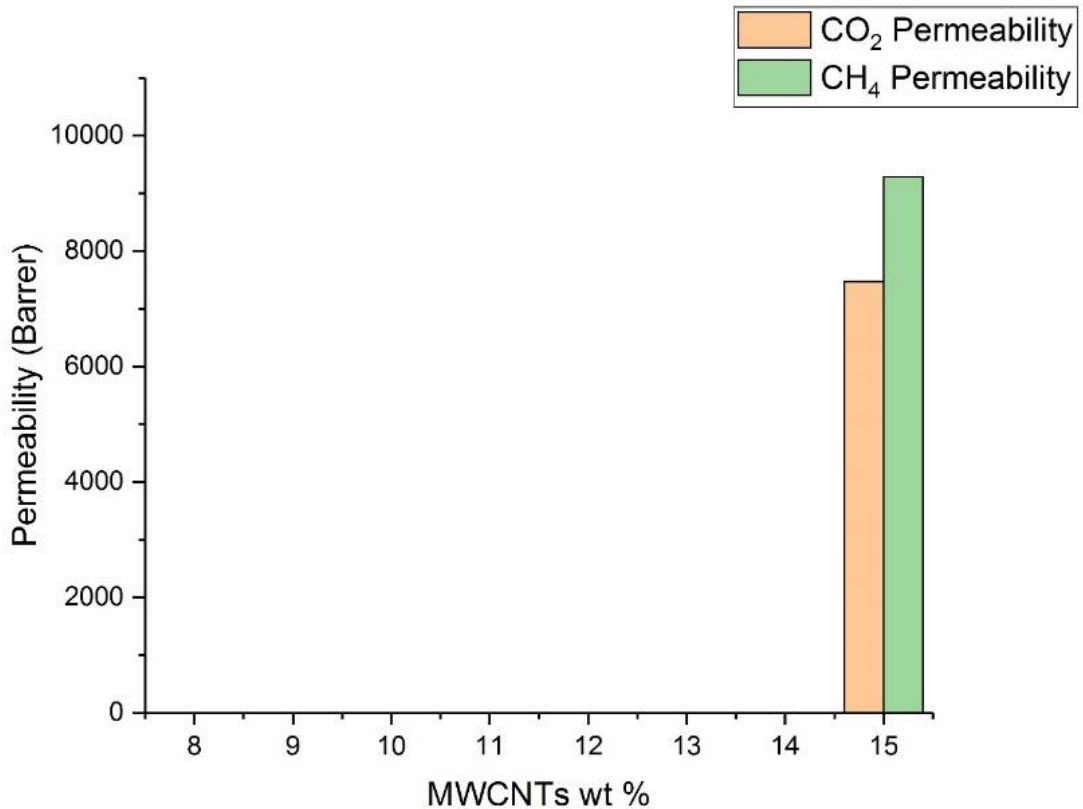


Figure 24: Permeabilities of MWCNTs/PA6 membranes in Phenol

As shown in above bar graph that trend for permeabilities are once again random, far from desirable behavior. As can be seen that permeabilities are so high for all CNTs wt% except for 15 wt% of CNTs. This trend is irregular and is indicative of some defect in membranes. Scanning electron microscopy has revealed that membranes have void which were created due to low thickness of base polymer PA6. Therefore, addition of MWCNTs require high thickness of membranes.

Figure 24 indicates that permeabilities of gases through membranes are very high in case of Mixed Matrix Membranes. At 8, 9, 10, 11, 12, 13, 14 wt% of MWCNTs in PA6, membranes synthesized were defective and had voids. The voids were observable in SEM and resulted in permeabilities so high which cannot be measured. However, membrane synthesized at 15 wt% were defect free and resulted in relatively lower permeabilities. Permeabilities were observed only at 15 wt% of carbon nanotube filler. The trend is irregular and therefore does not led to any conclusion.

5.2.3.1.4. Selectivities of MWCNTs/PA6 membranes in Phenol

Table 13: Selectivities of MWCNTs/PA6 membranes in Phenol

MWCNTs Weight %	α CO ₂ /CH ₄	α CH ₄ /CO ₂
8.00	-	-
9.00	-	-
10.00	-	-
11.00	-	-
12.00	-	-
13.00	-	-
14.00	-	-
15.00	0.80	1.24

Selectivity for 15 wt% MWCNTs/PA6 membrane are again very low which prohibits its industrial application as Mixed Matrix Membrane (MMM). Table 13 indicates selectivity of membranes with fillers v/s filler wt% as can be seen in above table that due to non-repeatability of experiments the data obtained is irregular and in some cases due to void formation, permeability is so high that it becomes practically unmeasurable. Since selectivities are dependent on permeabilities, the trend is random same as for permeabilities, as can be seen from above table. Also, this shows that at 15 wt % where permeabilities are relatively measurable, selectivities are not sufficient to constitute efficient separation. This trend is irregular and is indicative of some defect in membranes. Scanning electron microscopy has revealed that membranes have void which were created due to low thickness of base polymer PA6. Therefore, addition of MWCNTs require high thickness of membranes.

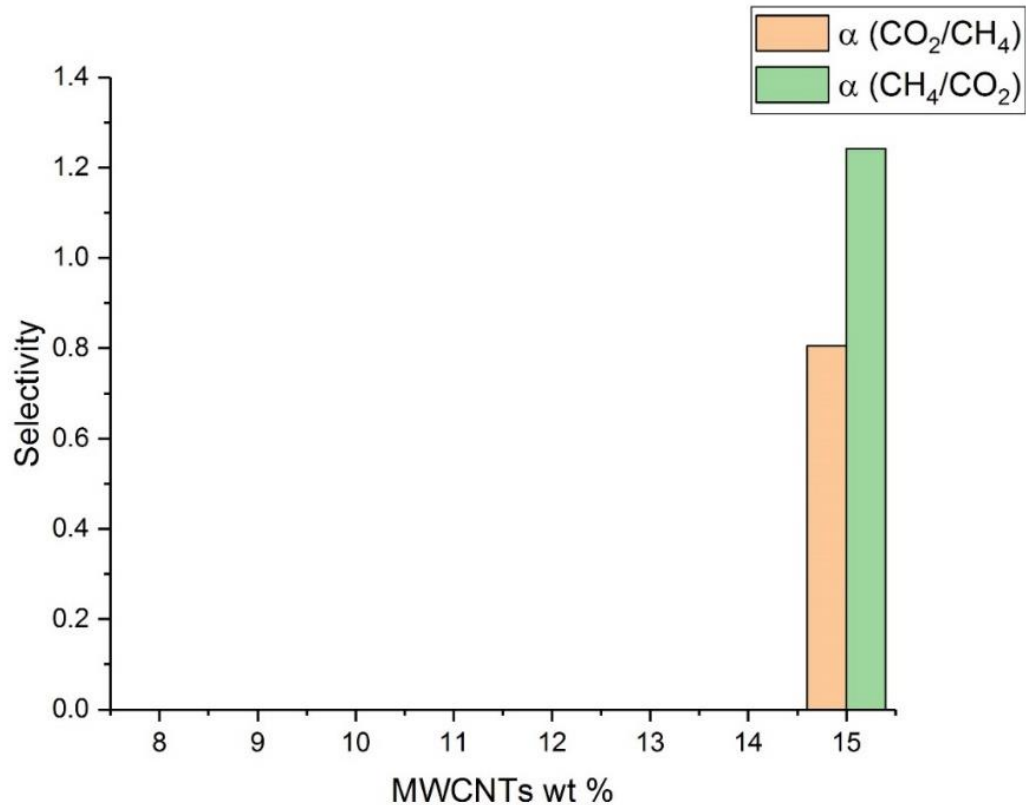


Figure 25: Selectivities of MWCNTs/PA6 membranes in Phenol

Selectivities of membranes for the purpose of reproducibility have shown the same irregular trend and are very low. Fig 25 indicates selectivity of membranes with fillers v/s filler wt% as can be seen in above table that due to non-repeatability of experiments the data obtained is irregular and in some cases due to void formation, permeability is so high that it becomes practically unmeasurable. Since selectivities are dependent on permeabilities, the trend is random same as for permeabilities, as can be seen from above figure. Also, this shows that at 15 wt % where permeabilities are relatively measurable, selectivities are not sufficient to constitute efficient separation. This trend is irregular and is indicative of some defect in membranes. Scanning electron microscopy has revealed that membranes have void which were created due to low thickness of base polymer PA6. Therefore, addition of MWCNTs require high thickness of membranes.

Permeation experiments were performed on the basis of three parameters.

- I. Pressure difference effect
- II. Membrane temperature effect
- III. Filler loading effect

5.2.4. Effect of pressure difference on gas permeability

The pure PA6 membrane shows very high permeability at low pressure ($\Delta P = 0.5$ bar). Permeability decreases with increase in pressure (Fig. 26). This is indicative of low energy consumption by membrane modules since it is giving output at very low pressure.

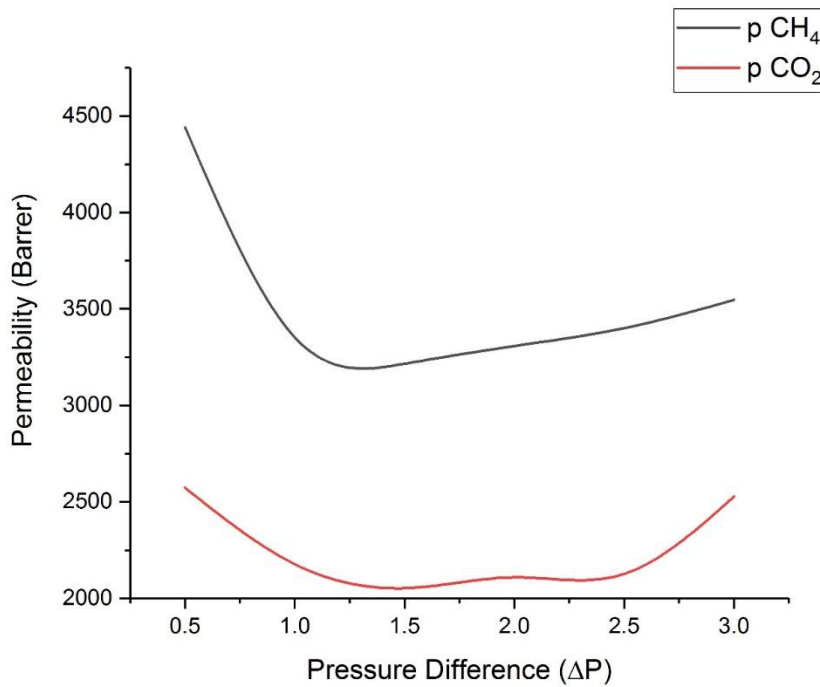


Figure 26: Effect of pressure difference on permeability ($T = 65$ °C)

In figure 26, permeability of gases CO_2 and CH_4 initially, decreases with increase in pressure difference. Pressure difference is the main driving force behind gas permeation. Permeation depends on pressure difference by the following formula:

$$P = \frac{QL}{\Delta PA}$$

Where Q = Gas flow rate

L = Thickness of membrane

A = Area of cross section

ΔP = Pressure difference

As can be seen from above equation that permeability is inversely proportional to pressure difference. So with increasing pressure difference, permeability decreases. The increase in permeabilities of gases after 2.0 bar pressure difference is because of increase flow rate Q due to high driving force (pressure difference). Therefore, it's the ratio of $(Q/\Delta P)$ which increased and resulted in high permeability.

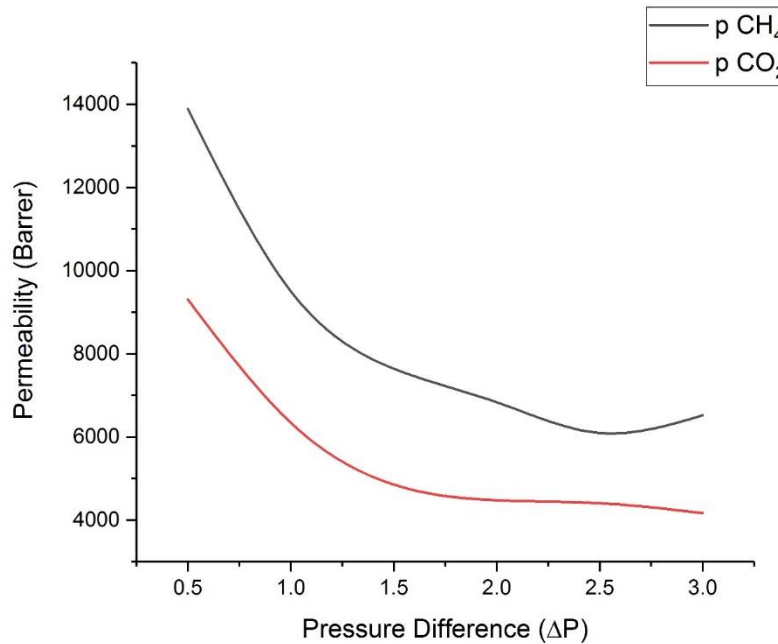


Figure 27: Effect of pressure difference on permeability ($T = 70 \text{ }^\circ\text{C}$)

Here the same behavior is observed as in the previous figure. The membrane is synthesized at a temperature of $70 \text{ }^\circ\text{C}$. With increasing driving force permeability decreases. The permeability is low at $\Delta P = 3.0$ bar and it is high at $\Delta P = 0.5$ bar. This indicates that high membrane has better performance at 0.5 bar and is thus energy efficient. Since high

pressure is applied through compressors, it requires energy. Therefore, high permeability at low pressure is desirable.

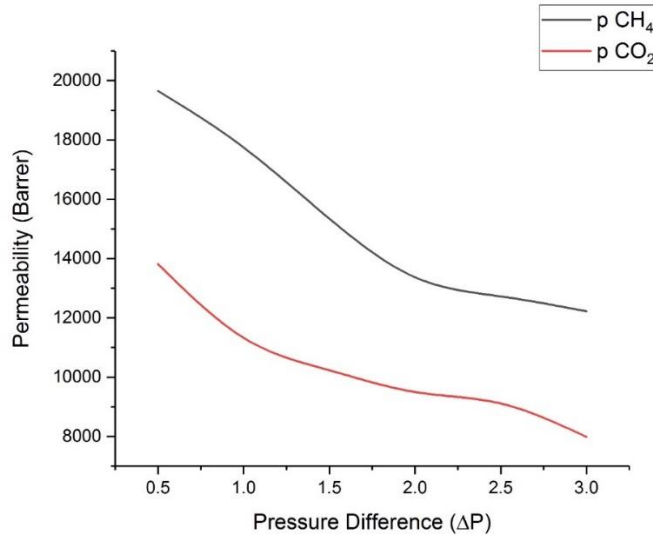


Figure 28: Effect of pressure difference on permeability ($T = 75\text{ }^\circ\text{C}$)

The membrane is synthesized at a temperature of $75\text{ }^\circ\text{C}$. With increasing driving force permeability decreases. The permeability is low at $\Delta P = 3.0$ bar and it is high at $\Delta P = 0.5$ bar. This indicates that high membrane has better performance at 0.5 bar and is thus energy efficient. Since high pressure is applied through compressors, it requires energy. Therefore, high permeability at low pressure is desirable.

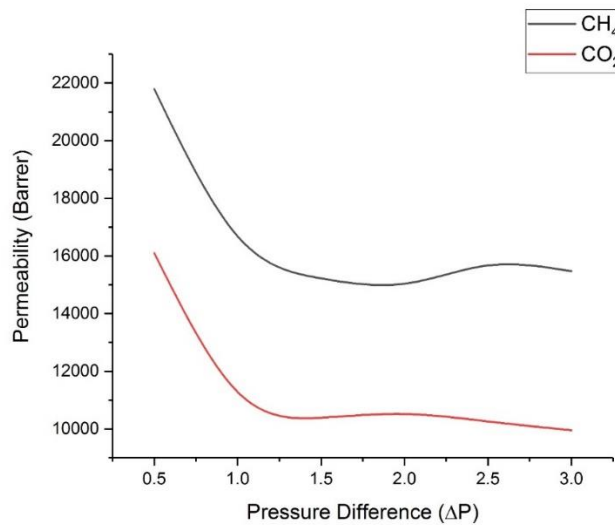


Figure 29: Effect of pressure difference on permeability ($T = 80\text{ }^\circ\text{C}$)

The membrane is synthesized at a temperature of 80 °C. With increasing driving force permeability decreases. The permeability is low at $\Delta P = 3.0$ bar and it is high at $\Delta P = 0.5$ bar. This indicates that high membrane has better performance at 0.5 bar and is thus energy efficient. Since high pressure is applied through compressors, it requires energy. Therefore, high permeability at low pressure is desirable. Above graphs show that with increasing pressure difference permeability decreases at every temperature of membrane synthesis.

5.2.5. Effect of temperature on gas permeability and selectivity

Permeability increases by increasing temperature. This is due to the free volume created due to high rate of solvent evaporation. In solution casting, free volume depends on rate of evaporation, slow evaporation means less permeable membrane and high selective membrane. PA6 has a disadvantage in this respect that it cannot be casted below its T_g . Below T_g membrane become brittle and breaks, which render it useless for practical purposes.

Table 14: Effect of Temperature on Permeability and Selectivity

Membrane	Temperature	ΔP (bar)	Selectivity		Permeability	
			α CO ₂ /CH ₄	α CH ₄ /CO ₂	p CO ₂	p CH ₄
Pure Nylon, 6	65	0.5	0.58	1.73	2,572	4,440
Pure Nylon, 6	70	0.5	0.67	1.49	9,302	13,886
Pure Nylon, 6	75	0.5	0.70	1.42	13,816	19,658
Pure Nylon, 6	80	0.5	0.74	1.35	16,098	21,786

Figure 30 indicates that permeability increases by increasing temperature of synthesis. This is due to the free volume created due to high rate of solvent evaporation. In solution casting technique, free volume depends on rate of evaporation, slow evaporation means less permeable membrane and high selective membrane. PA6 has a disadvantage in this respect that it cannot be casted below its T_g . Below T_g membrane become brittle and breaks, which render it useless for practical purposes. T_g of PA6 is around 47 °C and membrane has to be synthesized above 47 °C.

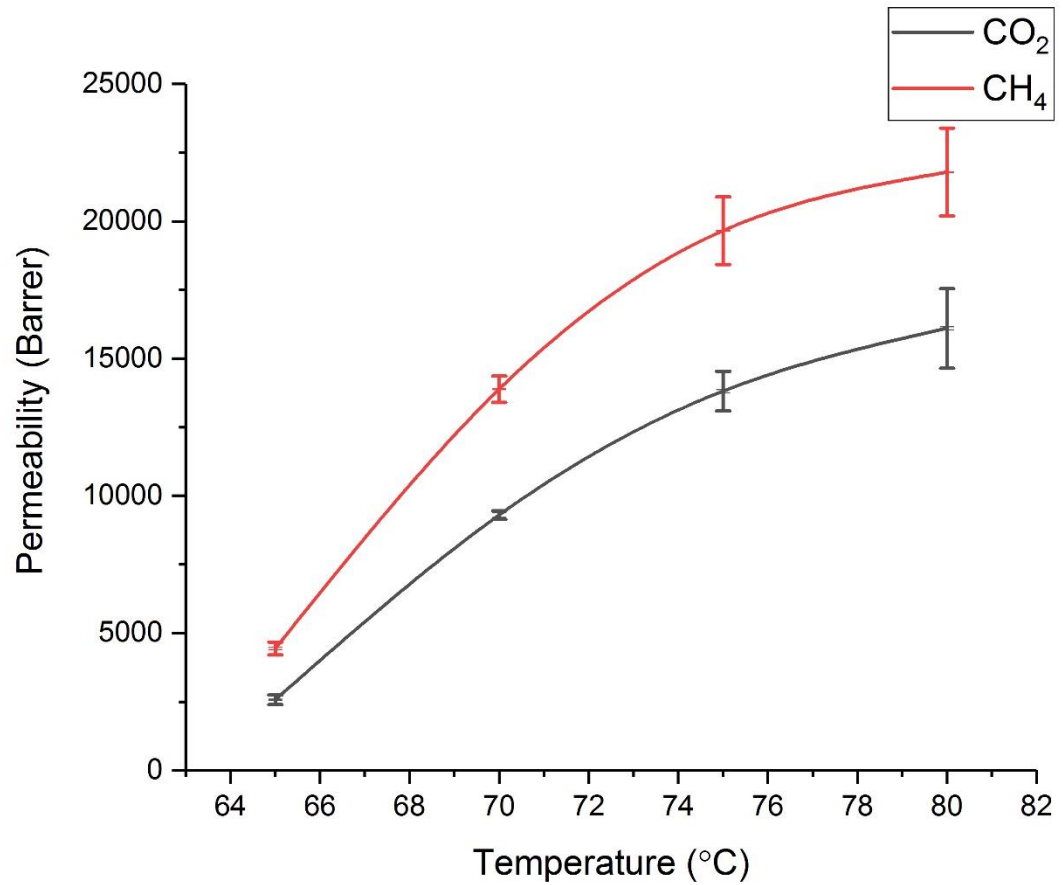


Figure 30: Effect of Temperature on permeability

5.2.6. Effect of filler loading on gas permeability and selectivity

Loading of filler decreases permeability but does not have any effect on selectivity. Carbon nanotubes dispersed in polymer matrix having thickness below 30 μm creates voids. This is due to agglomeration of carbon nanotubes in polymer matrix and also due to low threshold of stress of PA6 matrix. Increasing thickness of membranes results in high stress threshold of polymer and voids disappears. However, selectivity does not increase by adding carbon nanotubes which is due to the very high native permeability of PA6 membranes. Low selectivity is due to the fact stated by Robeson upper bound curve that with increasing permeability, selectivity decreases.

5.3. X-Ray Diffraction (XRD)

XRD graph of pure PA 6 membrane shows that Nylon 6 is glassy polymer. Sharp peak was obtained at 17.1° which shows the crystalline nature of PA6 membrane. Despite having crystalline nature, PA6 showed remarkable permeabilities of both CO_2 and CH_4 which is only possible in semi crystalline polymers. However, selectivity is very low for it to contribute to gas separation (Table 4). The sharp crystalline nature of polymer is due to its relatively high T_g at approx. 49°C . At room temperature (around 25°C), the polymer is below its glass transition temperature and thus crystalline in nature.

XRD showed one major peak at around 17.1° which is due to PA6.

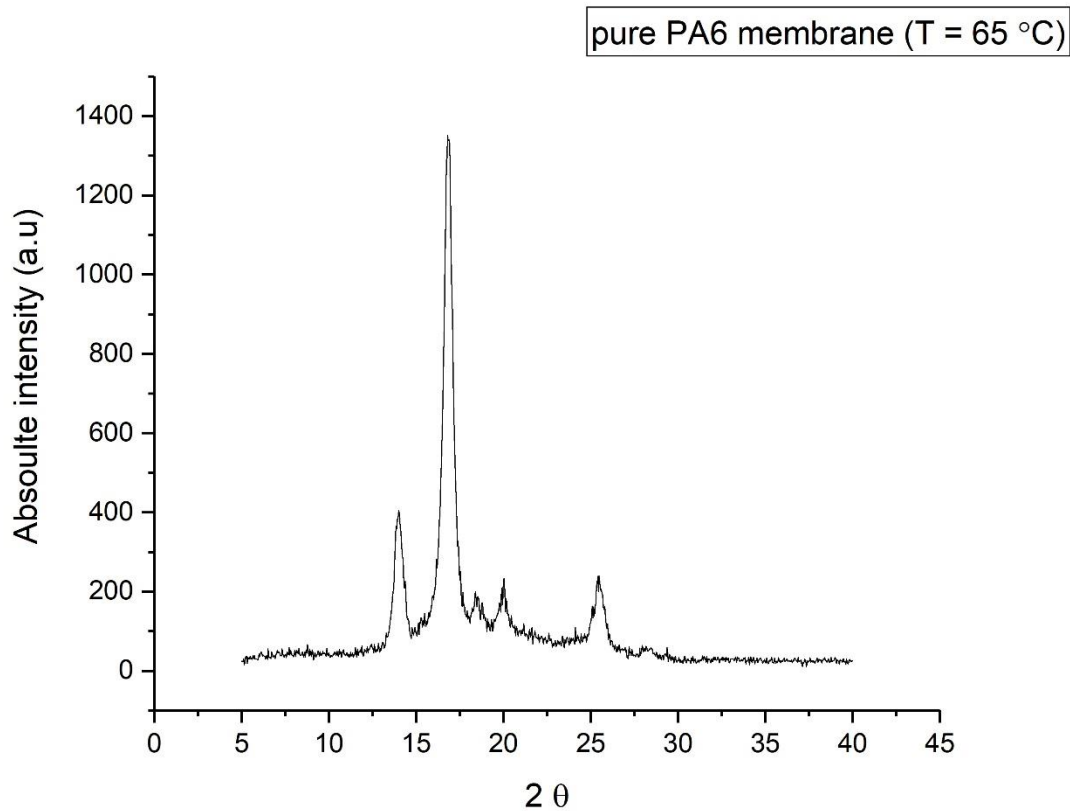


Figure 31: X-Ray Diffraction of pure PA6 membrane at $T = 65^\circ\text{C}$

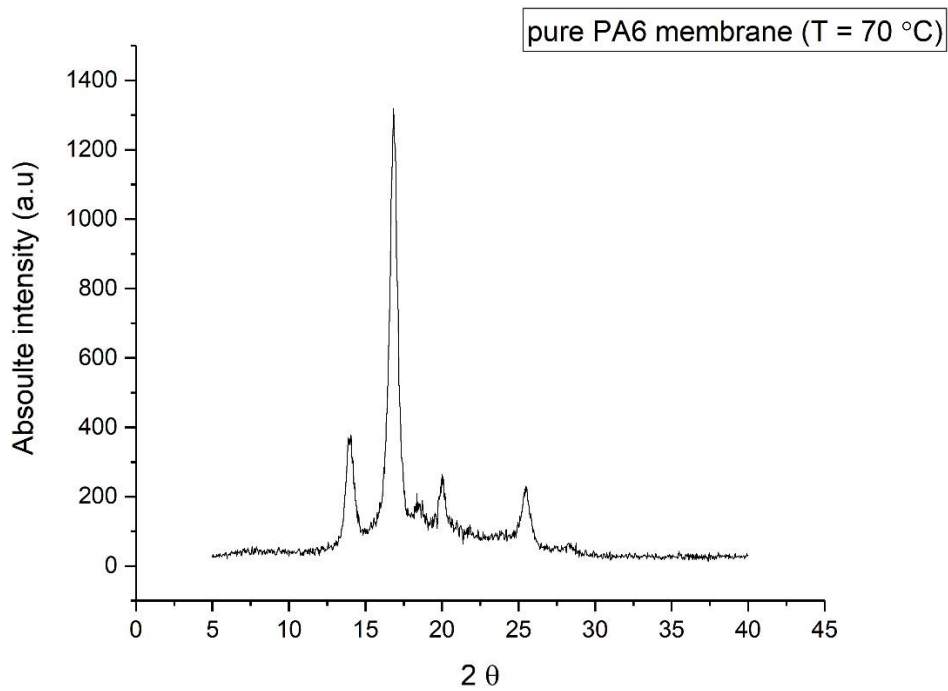


Figure 32: X-Ray Diffraction of pure PA6 membrane at T = 70 C

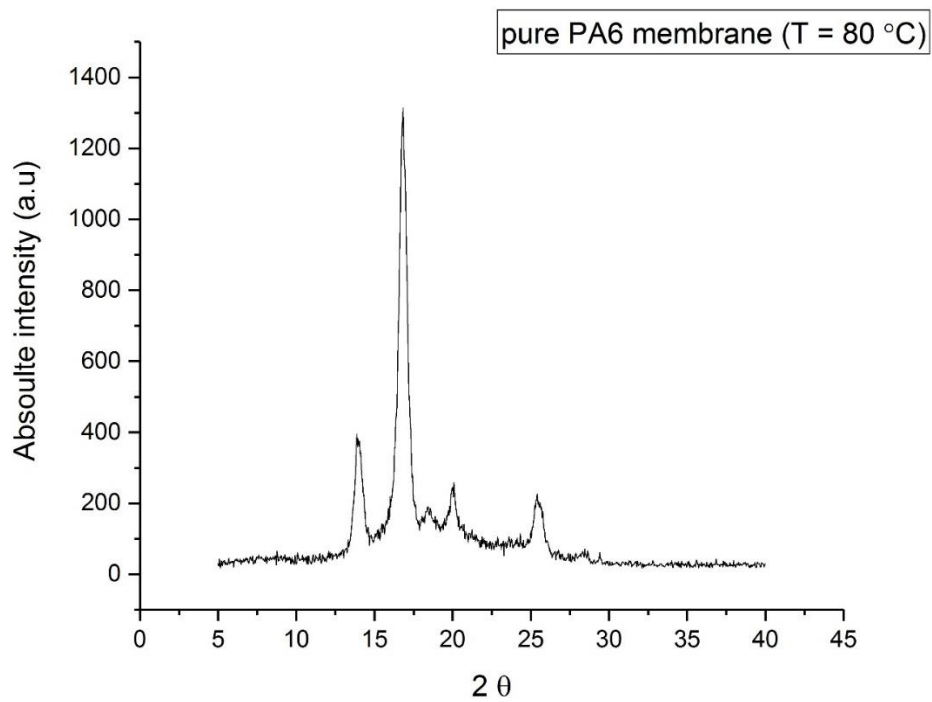


Figure 33: X-Ray Diffraction of pure PA6 membrane at T = 80 C

Figure 31 shows the x-ray diffraction of pure PA6 membrane at temperature of 65 °C. It indicates the sharp peak at 17 °C. Sharp peak indicates the crystalline nature of membrane. Figure 32 indicates the X-ray diffraction image at temperature of 70 °C. It also shows sharp peak at around 17 °C. Figure 33 shows the x-ray diffraction of pure PA6 membrane at 80 °C. Also it can be observed that membrane is crystalline which is evident from sharp peak at 17 °C. All above temperatures are temperature of oven at which membranes are synthesized. So 65 °C, 70 °C, 80 °C are synthesis temperatures. Since composition of polymer is same in all three samples specimen, X-ray imaging was almost same for all three samples. It also shows that changing temperature does not have any effect on crystallinity of membranes. So the membranes are remarkable in that they have high permeability and are also crystalline in nature. Usually crystalline materials have low permeability due to order packing of atoms. However, this material is a notable exception in that it has high permeability and also has crystalline structure.

5.4. Thermogravimetric Analysis

In TGA weight loss determines thermal stability of membranes. Weight loss of pure PA6 membrane starts at around 350 °C. At around 400 °C, final decomposition of membrane starts. Major weight loss occurs between 350 °C and 450 °C (Fig. 34 - 36). From weight loss, it is evident that PA6 is highly stable polymeric material as compared to some other polymers like Cellulose Acetate (CA) which starts thermal decomposition at around 250 °C. Thus, PA6 will remain stable for longer periods of time at higher temperature compared to cellulose acetate. TGA curves of membranes synthesized at 70 °C, 75 °C and 80 °C are shown in figures below. All figures show that approximately same behavior. It is evident from TGA results that synthesis temperature of membranes do not affect its thermal stability.

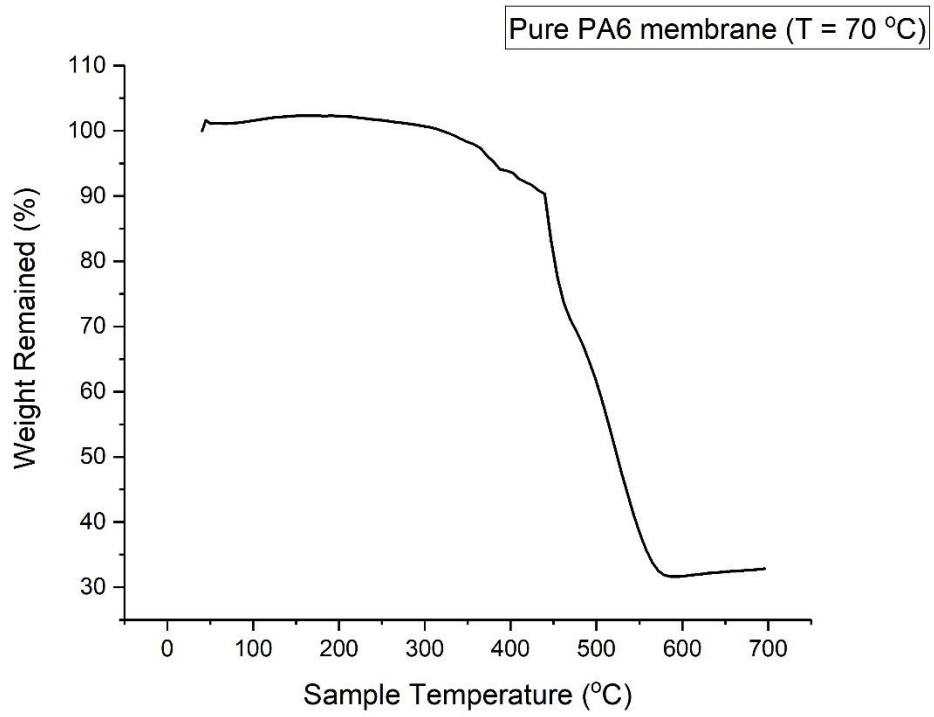


Figure 34: TGA Analysis of pure PA6 membrane synthesized at 70 °C

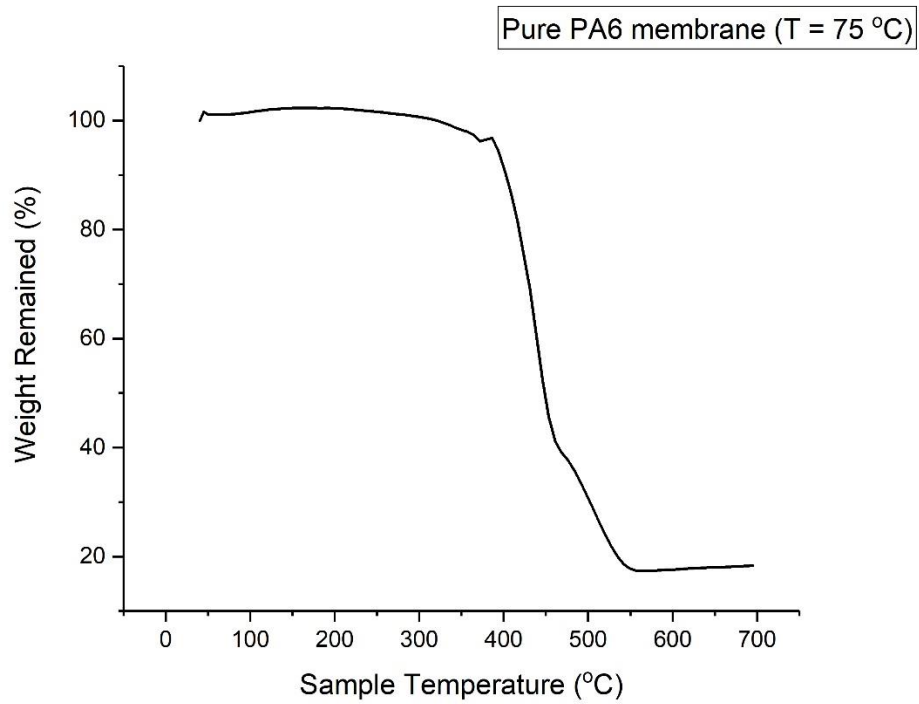


Figure 35: TGA Analysis of pure PA6 membrane synthesized at 75 °C

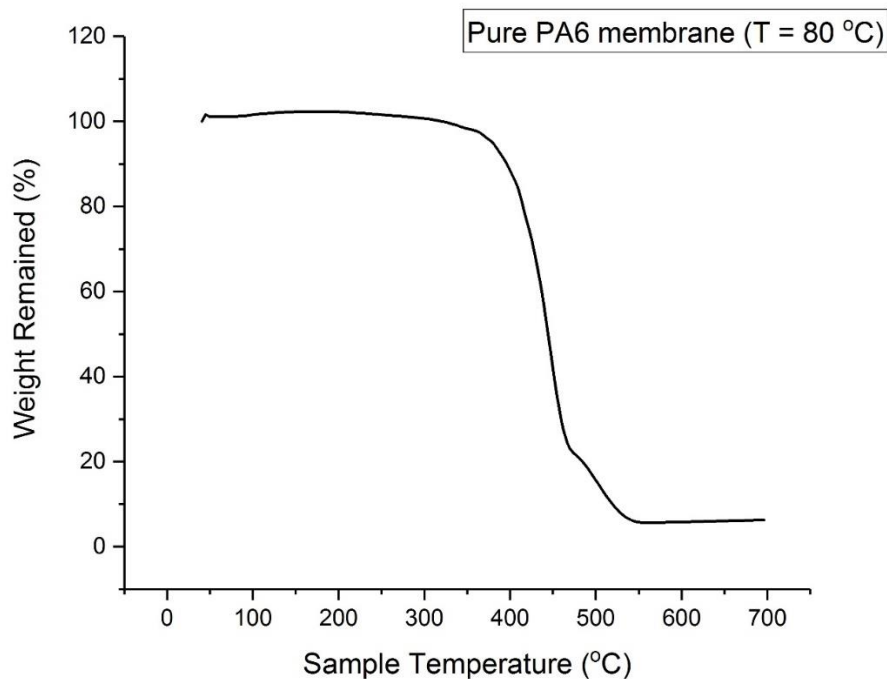


Figure 36: TGA Analysis of pure PA6 membrane synthesized at 80 °C

5.5. Tensile Testing

To investigate the mechanical properties of pure PA6 and PA6/MWCNTs, tensile testing on rectangular strips of fabricated membranes was carried out at room temperature. For this purpose, Universal Testing Machine (AG-XPlus Shimadzu) was used. The cross sectional area of specimens tested was 8.5mm and gauge length was 10 ± 0.5 mm.

(Fig. 37) indicates the relationship between stress and strain of pure PA 6 membranes, 10 wt% MWCNTs in Phenol and 10 wt% MWCNTs in Formic Acid. As can be seen that pure membrane can tolerate stress up to 21.5 N/mm^2 whereas strain shown is 25 %.

The behavior of membrane synthesized in phenol is different from that of pure membrane. Since membrane is being synthesized at higher temperature of 90 °C, slow evaporation occurs and membrane becomes denser and stiff. Also, addition of CNTs increased stiffness and decreased stress and strain of membrane. As can be seen in fig. membrane in phenol has maximum stress of around 16.1 N/mm^2 whereas strain has reduced to 8.28 %. The

membrane synthesized in formic acid is synthesized at low temperature of 70 °C. Since boiling point of Formic Acid is 100.8 °C, which is considerably less than that of phenol which is 181.7 °C, fast evaporation takes place in case of membrane synthesized from Formic Acid. This membrane however has low stress strain relationship than that of pure membrane and has peak value of 10 N/mm² of stress. The strain is 11.67 %. This is due to Carbon nanotubes embedded in polymer matrix.

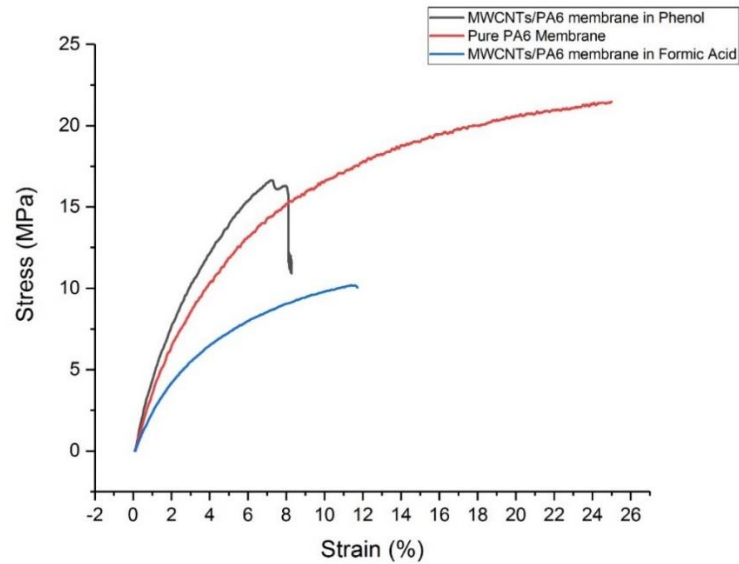


Figure 37: Stress vs Strain relationship of 10 wt% MWCNTs in phenol, Pure PA6 membrane, 10 wt% MWCNTs in Formic Acid

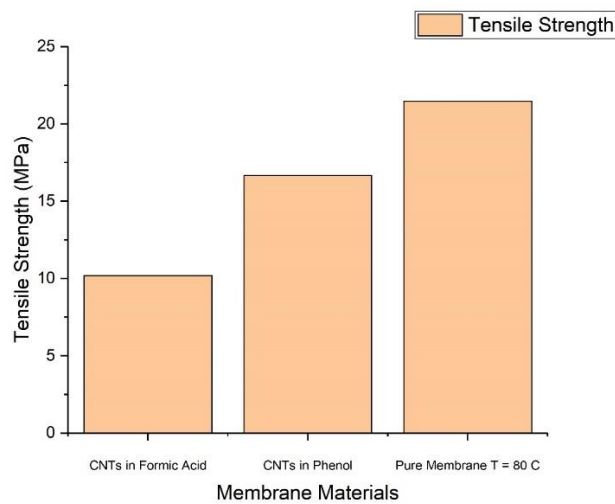


Figure 38: Tensile Strength of different membrane materials

(Fig. 38) indicates the relationship between different materials and membrane materials of pure PA 6 membranes ($T = 80\text{ }^{\circ}\text{C}$), 10 wt% MWCNTs in Phenol and 10 wt% MWCNTs in Formic Acid. As can be seen that pure membrane can tolerate stress up to 21.5 N/mm^2 . The behavior of membrane synthesized in phenol is different from that of pure membrane. Since membrane is being synthesized at higher temperature of $90\text{ }^{\circ}\text{C}$, slow evaporation occurs and membrane becomes denser and stiff. Also, addition of CNTs increased stiffness and decreased stress and strain of membrane. As can be seen in Fig. 38 membrane in phenol has maximum stress of around 16.1 N/mm^2 . The membrane synthesized in formic acid is synthesized at low temperature of $70\text{ }^{\circ}\text{C}$. Since boiling point of Formic Acid is $100.8\text{ }^{\circ}\text{C}$, which is considerably less than that of phenol which is $181.7\text{ }^{\circ}\text{C}$, fast evaporation takes place in case of membrane synthesized from Formic Acid. This membrane however has low stress than that of pure membrane and has peak value of 10 N/mm^2 of stress. This is due to Carbon nanotubes embedded in polymer matrix.

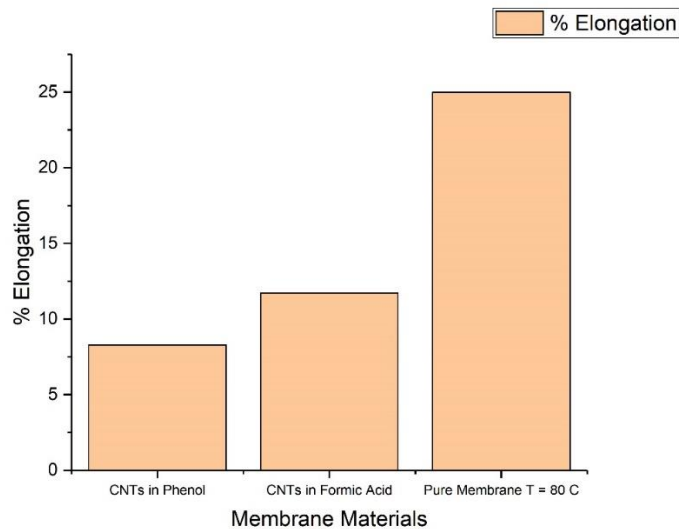


Figure 39: % Elongation of different membrane materials

(Fig. 39) indicates the relationship between different membrane materials and % elongation of pure PA 6 membranes ($T = 80\text{ }^{\circ}\text{C}$), 10 wt% MWCNTs in Phenol and 10 wt% MWCNTs in Formic Acid. As can be seen that pure membrane has strain of 25 %. The behavior of membrane synthesized in phenol is different from that of pure membrane. Since membrane is being synthesized at higher temperature of $90\text{ }^{\circ}\text{C}$, slow evaporation occurs and membrane becomes denser and stiff. Also, addition of CNTs increased stiffness and

decreased stress and strain of membrane. As can be seen in Fig. 39 membrane in phenol has strain reduced to 8.28 %. The membrane synthesized in formic acid is synthesized at low temperature of 70 °C. Since boiling point of Formic Acid is 100.8 °C, which is considerably less than that of phenol which is 181.7 °C, fast evaporation takes place in case of membrane synthesized from Formic Acid. This membrane has strain of 11.67 %.

Table 15: Mechanical Properties of different Membrane Materials

Membrane Materials	Tensile Strength (MPa)	% Elongation (%)
CNTs in Formic Acid	10.18524	11.7199
CNTs in Phenol	16.64956	8.285417
Pure Membrane (T = 80 °C)	21.47223	24.99656

5.6. Conclusion

In this study, pure PA6 and MWCNTs/PA6 composite membrane were synthesized at different temperatures and by using different solvents. The gases used for permeation studies were CO₂ and CH₄. Polyamide 6 is a very tough polymer and has high percentage elongation. Also, it is thermally stable at up to 350 °C. Binders like PEG cannot be used with base polymer for synthesis due to relatively high temperature require for membrane fabrication.

PA6 membranes were fabricated with average thickness of 27 µm at four different temperatures. Increasing temperatures of synthesis results in high gas permeabilities. Pure PA6 membrane also show remarkable behavior of high permeabilities at low pressure and it decreases with increase in pressure. This means that PA6 membranes can be utilized for low energy processes. Addition of CNTs do not have any effect on membrane selectivity but reduced its permeability. Therefore, utilization of PA6 membranes as an efficient Mixed Matrix membranes is very unlikely. Tensile testing of PA6 membrane showed that pure PA6 membrane has high stress and strain threshold and can be very flexible if sudden pressure changes in membrane module. However, addition of filler decreases both properties with membrane fabricated from phenol as a solvent showing better stress

threshold than that of membrane synthesized from Formic Acid. It can be concluded that with the exception of selectivity every other property of PA6 membrane is better than many commercial polymers like cellulose acetate. Therefore, any future work must focus on the preparation of composite membrane with PA6 being utilized as a dense support.

5.7. Future Recommendations

Permeabilities of pure PA6 membranes are very high at high temperature of synthesis. However, selectivities are low. Therefore, PA6 membranes can only be used as support for gas separation. Future studies must be focused on utilizing PA6 membrane as a dense support for gas separation. Also, functionalization of CNTs be incorporated to further test whether organic fillers work with PA6 polymer. For support membrane, thin selective membrane must be of material having high affinity with PA6 so that annealing can result in polymer binding.

Appendix – A

Membrane: a physical barrier to separate to separate component gases based on their affinity in membrane material

Permeate: components which pass through membrane

Retentate: components which do not pass through membrane

Mixed Matrix Membrane (MMM): membrane having blend of metal particles with polymer

Facilitated Transport Membranes (FTM): Membranes in which diffusion of components is facilitated by presence of water are called facilitated transport membranes.

Fixed Site Carrier Membranes (FSC): Membranes which contain functional groups (NH₂ or OH) helps the diffusion of components through the membrane and hence these membranes are called fixed site carrier membranes

Permeability Test System: Permeability test system is a semi-automated system which have the ability to determine the pressure difference across the membrane and the flow rate of feed, permeate and retentate which can be utilized to determine the permeability of the system

Membrane Casting: Process of spreading the prepared solution in the forms of sheets and evaporation of solvent to obtain a solvent free polymeric sheet is called membrane casting

Scanning Electron Microscopy (SEM): Characterization technique used to determine the surface morphology and cross sectional area of membrane.

Thermo gravimetric Analysis (TGA): Characterization technique to determine the thermal stability of membrane.

X-Ray Diffraction (XRD): Characterization technique to determine the crystallinity of material.

References

- [1] R.W. Baker, B.T. Low, Gas Separation Membrane Materials: A Perspective, *Macromolecules*, 47 (2014) 6999-7013.
- [2] M. Mulder, Basic principles of membrane technology: Kluwer Academic Publishers, 1996
- [3] J. K. Mitchell, "On the penetrativeness of fluids," *Journal of medical sciences*, 1830.
- [4] R. W. Baker, *Membrane Technology and Applications*, 2003.
- [5] D. Gomes, S. P. Nunes, and K. V. Peinemann, "Membranes for gas separation based on poly(1-trimethylsilyl-1-propyne)–silica nanocomposites," vol. 246, pp. 13-25, 2005.
- [6] S. Rafiq, L. Deng, and M. Hägg, "Role of Facilitated Transport Membranes and Composite Membranes for Efficient CO₂ Capture—A Review," *ChemBioEng Rev.*, vol. 3, no. 2, pp. 68–85, 2016.
- [7] N. M. José, L. A. S. de A. Prado, and I. V. P. Yoshida, "Synthesis, characterization, and permeability evaluation of hybrid organic–inorganic films," *J. Polym. Sci. Part B Polym. Phys.*, vol. 42, no. 23, pp. 4281–4292, 2004.
- [8] L. M. Robeson, "The upper bound revisited," *J. Memb. Sci.*, vol. 320, no. 1, pp. 390–400, 2008
- [9] A. R. Moghadassi, Z. Rajabi, S. M. Hosseini, and M. Mohammadi, "Fabrication and modification of cellulose acetate based mixed matrix membrane: Gas separation and physical properties," *J. Ind. Eng. Chem.*, vol. 20, no. 3, pp. 1050–1060, 2014.
- [10] S. Rafiq, L. Deng, and M. Hägg, "Role of Facilitated Transport Membranes and Composite Membranes for Efficient CO₂ Capture—A Review," *ChemBioEng Rev.*, vol. 3, no. 2, pp. 68–85, 2016.
- [11] J. M. S. Henis and M. K. Tripodi, "Composite hollow fiber membranes for gas separation: the resistance model approach," *J. Memb. Sci.*, vol. 8, no. 3, pp. 233–246, 1981.
- [12] P. Bernardo, E. Drioli, and G. Golemme, "Membrane gas separation: a review/state of the art," *Ind. Eng. Chem. Res.*, vol. 48, no. 10, pp. 4638–4663, 2009.
- [13] J. Li, S. Wang, K. Nagai, T. Nakagawa, and A. W. H. Mau, "Effect of polyethyleneglycol (PEG) on gas permeabilities and permselectivities in its cellulose acetate (CA) blend membranes," *J. Memb. Sci.*, vol. 138, no. 2, pp. 143–152, 1998.
- [14] T. Kim, B. Li, and M. Hägg, "Novel fixed-site–carrier polyvinylamine membrane for carbon dioxide capture," *J. Polym. Sci. Part B Polym. Phys.*, vol. 42, no. 23, pp. 4326–4336, 2004

- [15] L. Deng and M.-B. Hägg, "Carbon nanotube reinforced PVAm/PVA blend FSC nanocomposite membrane for CO₂/CH₄ separation," *Int. J. Greenh. Gas Control*, vol. 26, pp. 127–134, 2014.
- [16] A. S. Kovvali and K. K. Sirkar, "Carbon dioxide separation with novel solvents as liquid membranes," *Ind. Eng. Chem. Res.*, vol. 41, no. 9, pp. 2287–2295, 2002.
- [17] C. Cornelius, C. Hibshman, and E. Marand, "Hybrid organic-inorganic membranes," *Sep. Purif. Technol.*, vol. 25, no. 1, pp. 181–193, 2001.
- [18] A. L. Khan, X. Li, and I. F. J. Vankelecom, "Mixed-gas CO₂/CH₄ and CO₂/N₂ separation with sulfonated PEEK membranes," *J. Memb. Sci.*, vol. 372, no. 1, pp. 87–96, 2011.
- [19] M. M. Khan et al., "Enhanced gas permeability by fabricating mixed matrix membranes of functionalized multiwalled carbon nanotubes and polymers of intrinsic microporosity (PIM)," *J. Memb. Sci.*, vol. 436, pp. 109–120, 2013.
- [20] R. Gurdeep Chatwal and S. K. Anand, "Instrumental method of chemical analysis." Himalaya publishing House, 2002.
- [21] A. Raza, S. Farrukh, and A. Hussain, "Synthesis, Characterization and NH₃/N₂ Gas Permeation Study of Nanocomposite Membranes," *J. Polym. Environ.*, pp. 1– 10